Optimizing and validating a *Caenorhabditis elegans* model as a tool for assessing contaminant-induced oxidative stress and oxylipin signalling

by

Colleen Elizabeth Clarke

A thesis submitted to the Faculty of Graduate and Postdoctoral Affairs in partial fulfillment of the requirements for the degree of

Master of Science

in

Chemistry, with a Specialization in Chemical and Environmental Toxicology

Carleton University

Ottawa, Canada

Abstract

Oxidative stress (OS) is a physiological mechanism that is induced by pollutants and can lead to pathophysiological conditions. Pollutants may be activated by phase I metabolism enzymes, becoming more reactive, inducing additional OS. Paraquat-induced OS was measured in *Caenorhabditis elegans* that were modified to express CYP2E1—a human cytochrome P450 enzyme that bioactivates xenobiotics—in either their endoplasmic reticulum (erCYP2E1) or mitochondria (mtCYP2E1). Paraquat induced worm death, but deaths were reduced when worms were incubated in antioxidants. Reactive oxygen species significantly increased in mtCYP2E1 and wild-type worms, and significantly decreased in erCYP2E1 worms. These assays will validate a final OS testing method: monitoring global oxylipin production by tandem mass spectrometry. Oxylipins are potent signalling molecules in stress responses, and optimization efforts increased their detection by 66%. Further oxylipin testing will provide a mechanistic overview of the OS response which could explain differences in CYP2E1 isozyme activation.

Acknowledgements

Thank you to my supervisor, Amy Rand, and my mentor, Todd Harris, for your guidance and expertise in troubleshooting, lab techniques, and preparing presentations and reports. Thank you, Amy, for your kindness and understanding when I needed time outside the lab. Thank you, Todd, for your supportive words after I'd get messy results; your encouragement helped me feel hopeful for the next try.

Thank you to my Rand lab colleagues for your friendship, conversation, troubleshooting, and for helping me prepare figures and equipment for my experiments. Thank you to Keegan Harris for showing me lab techniques, for helping me fix my equipment setups, and for working together through both our degrees in the Rand lab. Thank you to Erin Lange for letting me use the figure you prepared for oxylipin metabolism. Thank you, Amanda Ameyaa-Sakyi, for your positivity, your help with optimizing assays, and for taking over the worms; they'll be in great hands with you!

Thank you to Jessica Hartman for generously donating *C. elegans* strains and *E. coli* OP50 to our lab. Thank you to the Bruin lab for giving me access to and training me on your fluorescence microscope. Thank you to everyone in the McMullin, Avis, Storey, and Hosseinian labs for helping me source equipment and materials whenever the worms stopped co-operating. I sincerely appreciate all your help, equipment, and expertise.

Thank you to the other Colleen C. in Chemistry, for being my twin and friend, and for working together through each phase of our theses. To my other colleagues in Steacie and Nesbitt: thank you for being a huge but fun and welcome distraction.

Thank you to my parents, Brian and Sandra, who have been there for me every day, giving me lots of support and encouragement. My degree and life would have been

much harder without you. Thank you to my aunt Gerry, for her mentorship and friendship. Since my undergraduate degree, you have created my happy place that I can visit to both focus on schoolwork and relax with you. Thank you, Eric and Crystal, for your enduring friendship and support, and for frequent calls that have kept me energized during an ongoing pandemic and some bouts of research difficulties. Thank you to my other loved ones, who have brought me joy and helped me in countless ways.

Finally, thank you to *C. elegans*, which is the best model organism ever.

Table of contents

List of abbreviations

4-HNE, 4-hydroxy-2-nonenal
APS, ammonium persulfate
ARA, arachidonic acid
ATP, adenosine triphosphate
BCA, bicinchoninic acid
BHT, butylated hydroxytoluene
BSA, bovine serum albumin
cDNA, complementary deoxyribonucleic acid
COX, cyclooxygenase
CYP, cytochrome P450
CYP2E1, cytochrome P450 2E1
DCF, 2',7'-dichlorofluorescein
dH_2O, distilled water
DHA, docosahexaenoic acid
DHET, dihydroxyeicosatrienoate
diH_2O, deionized water
DiHDPE, dihydroxydocosahexaenoate
DiHETE, dihydroxyeicosapentaenoate
DiHETrE, dihydroxyeicosatrienoate
DiHOME, dihydroxyoctadecadienoate
DMSO, dimethylsulfoxide
DNA, deoxyribonucleic acid
DNP, 2,4-dinitrophenyl
DNPH, 2,4-dinitrophenylhydrazine
DTT, dithiothreitol
ECL, enhanced chemiluminescence
EDTA, 2,2',2'',2'''-(ethane-1,2-diyldinitrilo)tetraacetic acid
EET, epoxyeicosatrienoate
ELISA, enzyme-linked immunosorbent assay
EPA, eicosapentaenoic acid
EpDPE, epoxydocosahexaenoate
EpETE, epoxyeicosapentaenoate
EpETrE, epoxyeicosatrienoate
EpFA, epoxy fatty acid
EpOME, epoxyoctadecadienoate
ER, endoplasmic reticulum
erCYP2E1, endoplasmic reticulum cytochrome P450 2E1
F_2-Iso-P, $PGF_{2\alpha}$–like isoprostane
GFP, green fluorescent protein
GST, glutathione S-transferase
H_2-DCF, 2',7'-dichlorodihydrofluorescein
H_2-DCFDA, 2',7'-dichlorodihydrofluorescein diacetate
HCl, hydrochloric acid

HDHA, hydroxydocosahexaenoate
HEPE, hydroxyeicosapentaenoate
HETE, hydroxyeicosatetraenoate
HODE, hydroxyoctadecadienoate
HpETE, hydroperoxyeicosatetraenoate
HPLC, high performance liquid chromatography
HRP, horseradish peroxidase
IgG, immunoglobulin G
Iso-P, isoprostane
L1, first larval stage
L2, second larval stage
L3, third larval stage
L4, fourth larval stage
LA, linoleic acid
LB, lysogeny broth
LC10, lethal concentration for 10% of the population
LC50, lethal concentration for 50% of the population
LC90, lethal concentration for 90% of the population
LC-MS, liquid chromatography-mass spectrometry
LOD, limit of detection
LOX, lipoxygenase
LT, leukotriene
MDA, malondialdehyde
mRNA, messenger ribonucleic acid
mtCYP2E1, mitochondrial cytochrome P450 2E1
NADPH, nicotinamide adenine dinucleotide phosphate
NAPQI, N-acetyl-p-benzoquinone imine
NGM, nematode growth medium
PFOA, Perfluorooctanoic acid
PG, prostaglandin
PUFA, polyunsaturated fatty acid
PVDF, polyvinylidene difluoride
qPCR, quantitative polymerase chain reaction
RNA, ribonucleic acid
RNAi, ribonucleic acid interference
ROS, reactive oxygen species
SDS, sodium dodecyl sulfate
SDS PAGE, sodium dodecyl sulfate polyacrylamide gel electrophoresis
sEH, soluble epoxide hydrolase
sEHI, soluble epoxide hydrolase inhibition
SOD, superoxide dismutase
TBARS, thiobarbituric acid reacting substances
TBST, Tris-buffered saline with Tween 20
TEMED, Tetramethylethylenediamine
UPLC-MS/MS, ultra performance liquid chromatography with tandem mass spectrometry

List of figures

List of tables

List of supplementary information

1.0 Introduction

1.1 Oxidative stress and distress

Oxidative stress is a critical physiological mechanism that is involved in redox signalling. Oxidative eustress is the maintenance of a physiological balance of oxidants and antioxidants [1]. However, if the system becomes unbalanced in the favour of oxidants, there will be an increased oxidant challenge (called oxidative distress) that disrupts redox signalling and control, or damages proteins, lipids, and DNA (deoxyribonucleic acid) [1].

1.1.1 Associated pathologies

Extensive oxidative damage to these macromolecules can result in organ failure and systemic disease. Oxidative distress may result in a variety of toxicological endpoints, including cardiovascular diseases, neurological diseases, carcinogenicity, diabetes, and rheumatoid arthritis [2]. One factor for increased oxidative distress and disease is exposure to environmental contaminants [2]. For example, the oxidative stress cause by styrene—an industrial compound used in the production of polystyrene—may play a role in lung carcinogenesis in mouse models [3]. Finally, while the epidemiological evidence linking the herbicide paraquat (1,1'-dimethyl-4,4'-bipyridinium) and Parkinson's disease remains inconclusive [4], paraquat exposure has been linked to neurotoxicity by oxidative stress in cell and mouse models [5, 6].

Given the association of oxidative stress with pathologies caused by environmental contaminants, the mechanism of oxidative stress induced by contaminants should be determined as one of the first steps in assessing chemical toxicity. Factors to study in the mechanism of oxidative stress by toxicants include reactive oxygen species (ROS) and

antioxidant proteins; and processes such as lipid peroxidation, protein carbonylation, and bioactivation of xenobiotics.

1.1.2 Reactive oxygen species

ROS are reactive oxygen-based chemicals involved in signalling and aerobic metabolism [1]. Table 1.1 provides a summary of radical and non-radical ROS [1].

Table 1.1 Radical and non-radical reactive oxygen species (ROS).

Free radicals	**Non-radicals**
Superoxide anion radical ($O_2^{\bullet-}$)	Hydrogen peroxide (H_2O_2)
Hydroxyl radical ($^{\bullet}OH$)	Organic hydroperoxide (ROOH)
Peroxyl radical ($^{\bullet}OOH$)	Singlet molecular oxygen ($O_2{}^1\Delta g$)
Alkoxyl radical ($RO^{\bullet}$)	Electronically excited carbonyls (RCO)
	Ozone (O_3)

Despite a name that implies that each of these molecules are very reactive, there are some ROS that are relatively stable. The least reactive ROS are the non-radical species, like hydrogen peroxide (H_2O_2) [1]. In reactions with the free amino acid methionine, H_2O_2 has one of the lowest rate constants of any ROS, at $2x10^{-2}$ L mol^{-1} s^{-1} [7]. Since H_2O_2 is more stable than other ROS, it is better able to diffuse away from its site of generation until reaching a more reactive biomolecule, acting as a second messenger [8]. In contrast, the hydroxyl radical ($^{\bullet}OH$) has the highest rate constant of any ROS, at $7x10^{9}$ L mol^{-1} s^{-1} [7]. The hydroxyl radical is so reactive that it has little specificity in its reactions; instead, it destroys almost any organic molecule it encounters [8]. There are a few ways H_2O_2 and other less reactive ROS can be transformed to more destructive ROS, like in reactions with transition metals and redox cycling.

Through Fenton and Haber-Weiss reactions with transition metals, H_2O_2 and the superoxide anion radical ($O_2^{\bullet-}$) (both of which are generated enzymatically) can be transformed into $^{\bullet}OH$ [9, 10].

$$Fe^{2+} + H_2O_2 \rightarrow Fe^{3+} + \bullet OH + OH^- \text{ (Fenton reaction 1)}$$

$$Fe^{3+} + H_2O_2 \rightarrow Fe^{2+} + \bullet OOH + H^+ \text{ (Fenton reaction 2)}$$

$$O_2^{\bullet-} + H_2O_2 \xrightarrow{Fe^{2+}} \bullet OH + OH^- + O_2 \text{ (Haber-Weiss reaction)}$$

In these reactions, the reactants are converted to other ROS, like $^{\bullet}OH$, the peroxyl radical ($^{\bullet}OOH$), and molecular oxygen (O_2). Each of these products are more reactive than H_2O_2, so the Haber-Weiss reaction would result in increased oxidative damage to surrounding tissue [7].

1.1.3 Redox cycling

Another way ROS are converted between one another is through redox cycling, where some aromatic compounds gain an electron just to donate it to O_2, forming $O_2^{\bullet-}$ in the process. Paraquat, a standard inducer of oxidative stress in models, undergoes redox cycling *in vivo*, a process that has two damaging consequences.

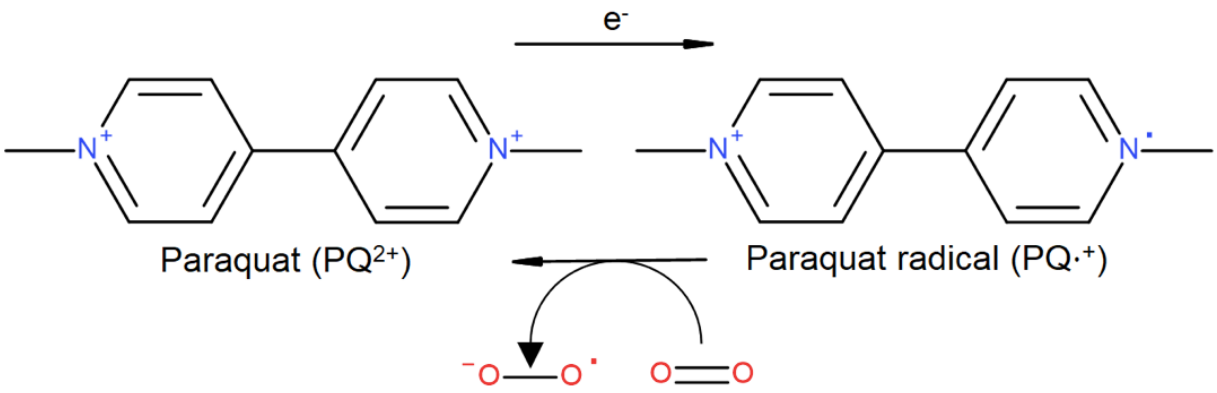

Figure 1.1 Paraquat undergoes redox cycling *in vivo*, depleting cellular reducing equivalents and generating superoxide from molecular oxygen.

First, paraquat is reduced by an electron donor, depleting the cell's reducing equivalents (like NADPH, or nicotinamide adenine dinucleotide phosphate) that are necessary for maintaining physiological levels of oxidative stress [11]. Second, paraquat donates the electron to molecular oxygen (O_2), catalyzing the formation of $O_2^{\bullet-}$ [11]. Through additional reactions, $O_2^{\bullet-}$ goes on to form other ROS that damage biological macromolecules. Meanwhile, non-radical paraquat has been regenerated and the production of radical ROS begins again.

1.1.4 Antioxidant proteins

Many proteins are involved in the cell's response to oxidative stress. ROS can transform to less destructive species when their radicals are scavenged by an antioxidant molecule, or they are transformed by antioxidant proteins. Antioxidant proteins may directly detoxify ROS, like SOD (which converts $O_2^{\bullet-}$ to H_2O_2) and catalase (which converts H_2O_2 to H_2O and O_2) [12]. They may also scavenge ROS directly, like heme oxygenase-1 (which catalyzes the degradation of free heme, producing carbon monoxide, iron, and biliverdin) [12]. Finally, phase II metabolism enzymes help eliminate oxidative xenobiotic compounds from the cell. For example, glutathione S-transferase catalyzes

the conjugation of endogenous compounds with glutathione—a soluble protein—allowing for their elimination from the cell) [12]. Antioxidant proteins counteract oxidative stress at physiological conditions, but their levels may be altered during oxidative distress.

Their expression may increase or decrease when a biological system undergoes increased oxidative stress. For example, when a cell in *Caenorhabditis elegans* (a roundworm)—is exposed to an oxidizing agent, ROS production increases and affects antioxidant gene expression (see Figure 1.2) [2].

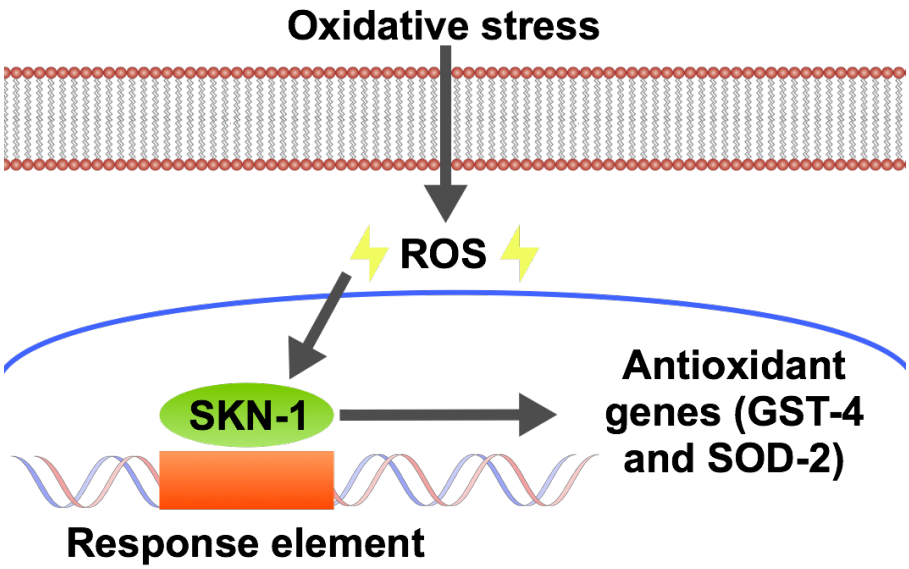

Figure 1.2 Reactive oxygen species (ROS) activate SKN-1—an oxidative stress response transcription factor—causing the upregulation of antioxidant genes.

If ROS are overproduced or if there are electrophiles in the cell, the degradation of SKN-1 (the *C. elegans* ortholog of mammalian Nrf2—a transcription factor for antioxidant genes) is inhibited [13]. This inhibition allows for the translocation of SKN-1 to the nucleus, where it initiates the transcription of various antioxidant response genes, including glutathione S-transferase-4 (GST-4) and superoxide dismutase-2 (SOD-2) [13]. Oxidative stress affects the expression of these enzymes, meaning that oxidative stress can be assessed by examining antioxidant gene expression levels.

1.1.5 Protein carbonylation

Protein carbonylation is another factor to study while investigating the oxidative stress mechanism. Protein carbonylation is the introduction of a carbonyl group—an aldehyde or a ketone—to proteins through the oxidation of amino acid residues [14]. Fenton reagents (H_2O_2 and Fe(II)) oxidize proteins directly to add carbonyl groups, with arginine, lysine, histidine, and proline being the amino acids most affected [14, 15]. Protein carbonylation can also result indirectly from the oxidation of lipids by $^{\bullet}OH$ [15].

1.1.6 Lipid peroxidation

The oxidation of polyunsaturated fatty acids (PUFA) like arachidonic acid (ARA) and linoleic acid (LA) starts a chain reaction called lipid peroxidation. The hydroxyl radical initiates the chain reaction by abstracting an electron from a lipid, then lipid radicals abstract electrons from other lipids and destroy tissue until the chain is broken [16]. Lipid peroxidation begins with the initiation step, where $^{\bullet}OH$ or another radical pro-oxidant abstracts an electron from a lipid (see Figure 1.3) [16]. These lipids then react with oxygen to form lipid peroxy radicals [15]. The next step is propagation, where the lipid peroxy radicals abstract electrons from other unsaturated lipids, producing a lipid hydroperoxide and another lipid radical [16]. The cycle continues until the final step: termination by an antioxidant. When ROS are at homeostatic cellular concentrations, the antioxidant defense system and antioxidant proteins are enough to terminate lipid peroxidation [16].

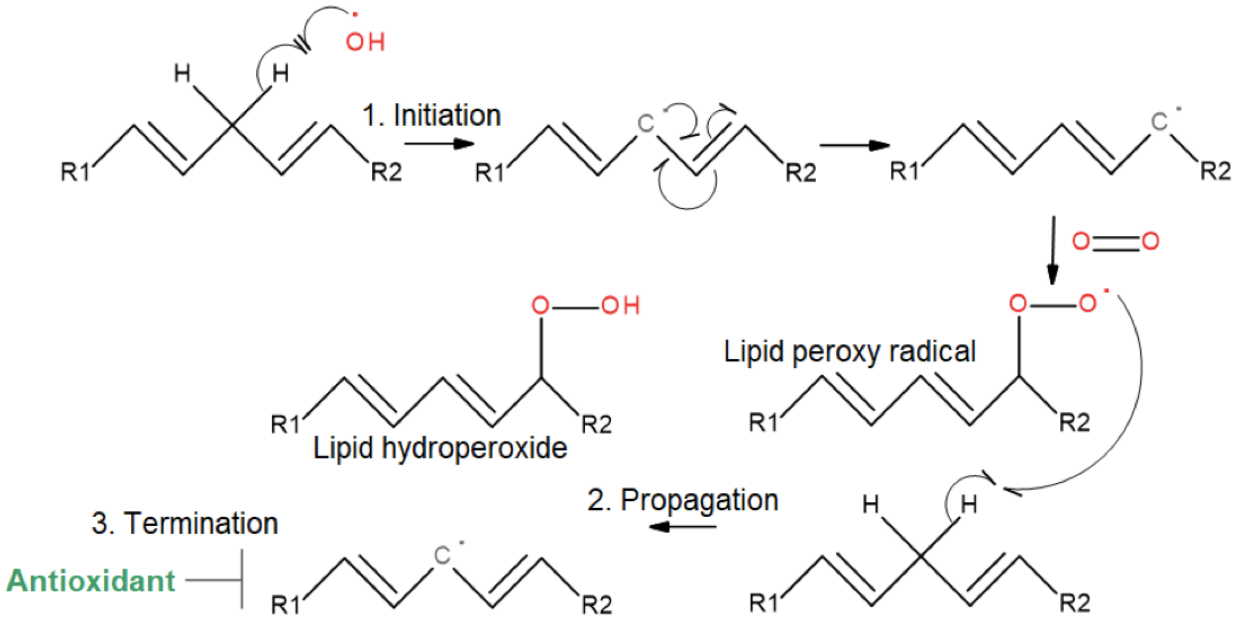

Figure 1.3 Reactive oxygen species like hydroxyl radicals initiate lipid peroxidation. The resulting lipid peroxy radical propagates the cycle by abstracting a proton from another lipid. The peroxidation continues until termination by an antioxidant.

When there is high lipid peroxidation, the oxidative damage to cell membranes is irreparable and the affected cells induce programmed cell death [16]. Some of the byproducts of lipid peroxidation add to its toxicity; as lipid hydroperoxides degrade, they form a variety of compounds (Figure 1.4), including isoprostanes (if the initial PUFA is ARA), conjugated dienes, and aldehydes like malondialdehyde (MDA) and 4-hydroxy-2-nonenal (4-HNE).

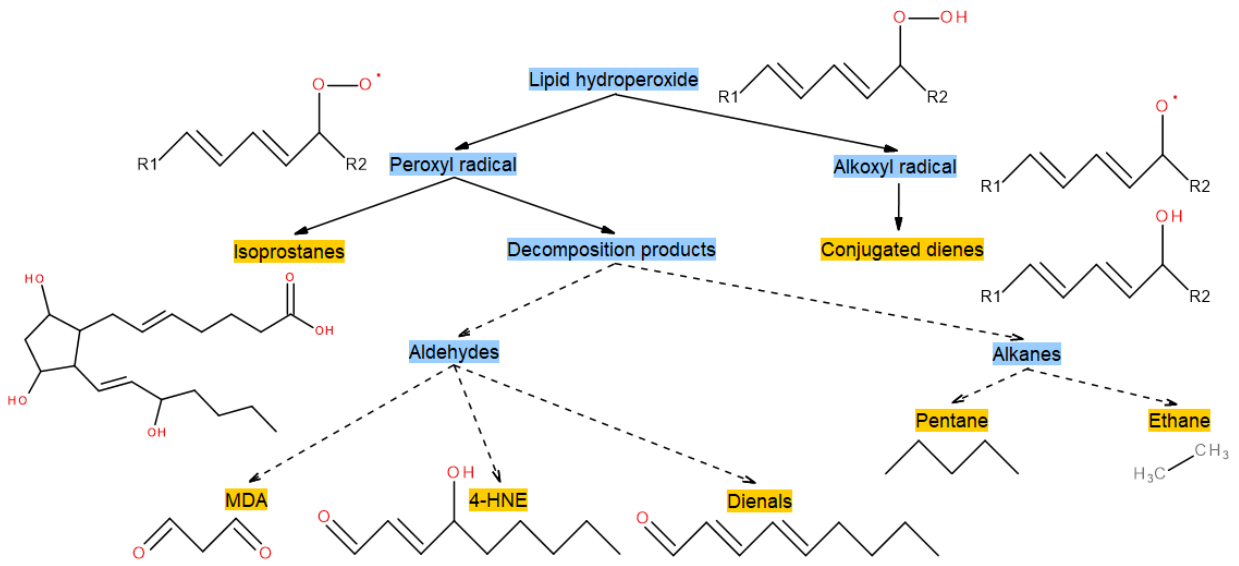

Figure 1.4 Lipid hydroperoxides degrade to form conjugated dienes, isoprostanes (if the starting fatty acid was arachidonic acid), alkanes, and aldehydes (adapted from Dotan et al. [17]).

Aldehydes are especially toxic because they are electronegative, making them more likely to react with nucleophilic biological macromolecules like proteins and DNA [18]. 4-HNE is the most cytotoxic by-product of lipid peroxidation and MDA is the most mutagenic [16, 19]. Each of the by-products mentioned above can be quantified to measure the extent of lipid peroxidation (with the different methods of quantification are explained in section 1.2.5).

1.1.7 Bioactivation of xenobiotics

Bioactivation—the biotransformation of a chemical, catalyzed by an enzyme—is a final important factor in studying the mechanism of oxidative stress [20]. Enzymes like cytochrome p450s (CYP), glucuronyl transferases, and peroxidases transform their substrates to more polar compounds [20]. Bioactivation reactions can activate drugs to target specific biomolecules, or detoxify xenobiotics [20] However, in some cases, the chemical may become activated to a chemically reactive electrophilic or radical product

that is even more toxic than the starting compound [20]. For example, acetaminophen is a pain-relief drug that is therapeutic at low doses. Once it is bioactivated by CYPs, it gets transformed to the more reactive N-acetyl-p-benzoquinone imine (NAPQI) [21]. NAPQI binds to proteins, leading to increased oxidative stress, DNA fragmentation, and eventually necrosis [22]. Acetaminophen overdose, because it is bioactivated to a more reactive compound, is the leading cause of acute liver failure in many Western countries [23]. Therefore, when using a cell or animal model to study oxidative stress, it is crucial that the model expresses metabolic enzymes that are like those of humans.

1.2 Cytochrome P450 2E1

Cytochrome P450 2E1 (CYP2E1) is a human phase I metabolism enzyme that is involved in drug and toxicant metabolism [24]. CYP2E1 acts as a monooxygenase (it adds an oxygen atom to its substrate), producing a metabolite that is more polar and water-soluble, and is therefore easier to excrete [24]. CYP2E1 metabolizes several small organic compounds like ethanol, acetaminophen, styrene, carbon tetrachloride, and chloroform [25, 26]. Unfortunately, CYP2E1 can also activate biologically inert compounds to form electrophilic metabolites that increase oxidative stress [25]. For example, during the metabolism of styrene, the heme center of CYP2E1 imparts an oxygen atom to compound, creating styrene oxide (Figure 1.5) [26, 27].

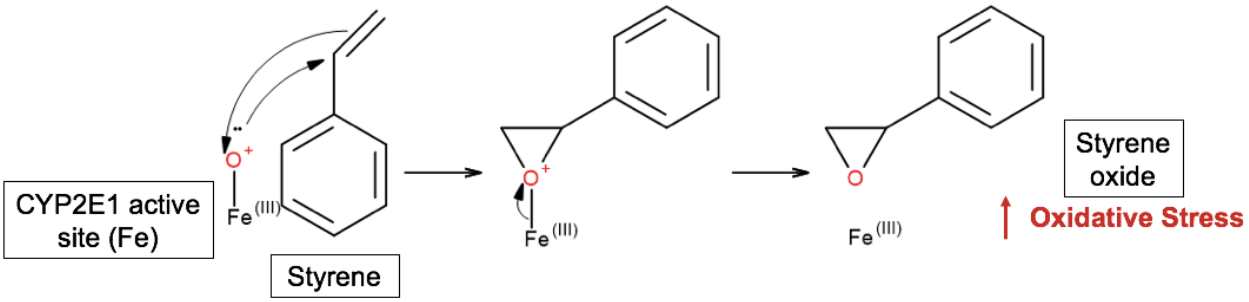

Figure 1.5 CYP2E1 metabolizes styrene to styrene oxide. The newly-formed epoxide group of styrene oxide is electrophilic, so it reacts more readily with biological nucleophiles.

The epoxide group on styrene oxide is electrophilic, so it can covalently react with and modify biological nucleophiles like proteins, DNA, and RNA [25]. Both styrene and styrene oxide have been associated with increases in ROS and SOD expression, so both are implicated in oxidative stress [3]. However, in mice lacking the enzyme that degrades styrene oxide (microsomal epoxide hydrolase-deficient), oxidative stress caused by styrene was increased [28]. The increased oxidative stress indicates that the bioactivation of styrene to an epoxide increases the compound's toxicity. Therefore, CYP2E1 is a potent source of oxidative stress through bioactivation.

CYP2E1 can also increase oxidative stress through uncoupling—with or without a substrate [27]! After CYP2E1 binds to its substrate (or even without a bound substrate), it gains an electron and binds to molecular oxygen [27]. The structure can rearrange to hold the electron on oxygen, creating $O_2^{\bullet-}$ that is bound to the enzyme's heme active site [27]. However, $O_2^{\bullet-}$ can occasionally break from the active site, resulting in free $O_2^{\bullet-}$ and regenerating the starting enzyme [27]. Alternatively, a second electron may be added prior to the degradation of $O_2^{\bullet-}$, which may result in free $^{\bullet}OOH$ [27]. Free $^{\bullet}OOH$ would then be reduced to make a third ROS, H_2O_2 [27]. Each of these ROS have been produced by

CYP2E1 without the addition of oxygen to any substrate, so even the presence of CYP2E1 and its uncoupled reactions can increase an organism's oxidative stress.

1.2.1 Cellular localization

Since CYP2E1 itself can increase oxidative stress, its location in the cell could also affect the extent of its toxicity. CYP2E1 is found in both the endoplasmic reticulum (ER) and the mitochondria, though most studies focus on endoplasmic reticulum CYP2E1 (erCYP2E1) [29]. Less is known about the importance of mitochondrial-localized CYP2E1 (mtCYP2E1), though there are some ideas about how and why CYP2E1 is targeted to the mitochondria.

The phosphorylation of the newly-synthesized CYP2E1 polypeptide at Ser-129 by Protein Kinase A has been proposed as part of the mechanism behind the localization of mtCYP2E1 [29]. Once the protein is phosphorylated, it activates a cryptic mitochondrial targeting signal between amino acids 21-31, resulting in the polypeptide being trafficked to the mitochondria [30]. The polypeptide is then folded, along with heme, into its final structure and deposited into the mitochondrial inner membrane [29]. About 20-25% of mtCYP2E1 are phosphorylated—suggesting a dynamic equilibrium of phosphorylation in the mitochondria—versus any phosphorylated erCYP2E1 being immediately destroyed by proteolysis [29]. This mechanism explains how CYP2E1 is in the mitochondria, but the purpose of CYP2E1 in the organelle is unclear.

The subcellular localization and post-translational modifications of CYP2E1 impact the isozymes' conformational states, and therefore their activity and affinity for certain substrates [31]. For example, while mtCYP2E1 follows Michaelis-Menten kinetics in the transformation of certain small organic molecules, erCYP2E1 does not [32].

Different enzyme activities imply different clearance rates—something that could have major consequences in both metabolism of endogenous and exogenous substrates.

1.2.2 Mitochondrial dysfunction and toxicity

The bioactivation of these substrates by CYP2E1 may result in mitochondrial dysfunction, which occurs when more damage has been done to the mitochondria (for example, to mitochondrial DNA, proteins, and lipids) than can be repaired [29]. It can result in insufficient adenosine triphosphate (ATP, or energy stores), an imbalance in ROS production, or alterations in other critical mitochondrial functions [29]. Many metabolites of CYP2E1 have been linked with mitochondrial dysfunction. For example, NAPQI—the product of acetaminophen metabolism by CYP2E1—depolarizes the inner mitochondrial membrane and reduces oxygen consumption in COS-7 monkey kidney fibroblast cells [33]. Both these effects are signs of mitochondrial dysfunction. CYP2E1-mediated metabolism is also a major factor in the bioactivation of carbon tetrachloride and the resulting mitochondrial dysfunction [34]. First, carbon tetrachloride is transformed to a trichloromethyl radical, which is then converted to a trichloromethyl peroxy radical [34]. Male albino Wistar rats exposed to these chemicals showed signs of mitochondrial dysfunction (specifically, impaired mitochondrial ultrastructure and inhibited mitochondrial enzymes) [35]. CYP2E1 is clearly involved in mitochondrial dysfunction, though it's possible that one isozyme drives the dysfunction more than its counterpart.

Given its location in the mitochondria, it's probable that mtCYP2E1 uncoupling results in more mitochondrial dysfunction than erCYP2E1. While there have not been studies about the extent of mtCYP2E1 uncoupling compared to that of erCYP2E1, there is evidence showing that mtCYP2E1 drives mitochondrial dysfunction through substrate

activation. In the earlier example with mitochondrial dysfunction in COS-7 cells exposed to acetaminophen, there was no significant difference between COS-7 cells expressing only mtCYP2E1 and cells expressing both erCYP2E1 and mtCYP2E1 [33]. With less overall CYP2E1 activity in the mtCYP2E1 COS-7 cells, it is possible that mtCYP2E1 plays a greater role in mitochondrial dysfunction than erCYP2E1 [33]. *In vivo* evidence linking mtCYP2E1 with mitochondrial dysfunction is in mice after exposure to 1,3-butadiene (a chemical in cigarette smoke) [36]. MtCYP2E1 was correlated with reductions in the activity of respiratory complexes I, II, III, and IV, whereas erCYP2E1 was not [36]. The combination of these *in vitro* and *in vivo* links between mtCYP2E1 and mitochondrial dysfunction provides strong evidence that mtCYP2E1 drives the toxicity of CYP2E1.

1.3 Testing methods for oxidative stress

Once a test organism is exposed to paraquat, styrene, or another pro-oxidant, oxidative stress can be measured in multiple ways, including conducting live assays with rescue by antioxidants or ROS-staining; monitoring individual markers of oxidative stress, like proteins involved in the oxidative stress response; measuring protein carbonylation; monitoring an array of proteins and genes (proteomics and genomics, respectively); measuring lipid peroxidation by quantifying 4-HNE production; and monitoring the production of multiple lipids (lipidomics).

1.3.1 Live assays

Live oxidative stress assays provide the most accurate results because they are non-invasive. Since the organism remains whole, there are no artifacts introduced from sample preparation (for example, from grinding samples in oxygenated air). The most accurate way to study the toxicokinetics of an organism is by keeping it alive. For these

reasons, assays requiring a whole organism—like survival, rescue, and fluorescence assays—are common.

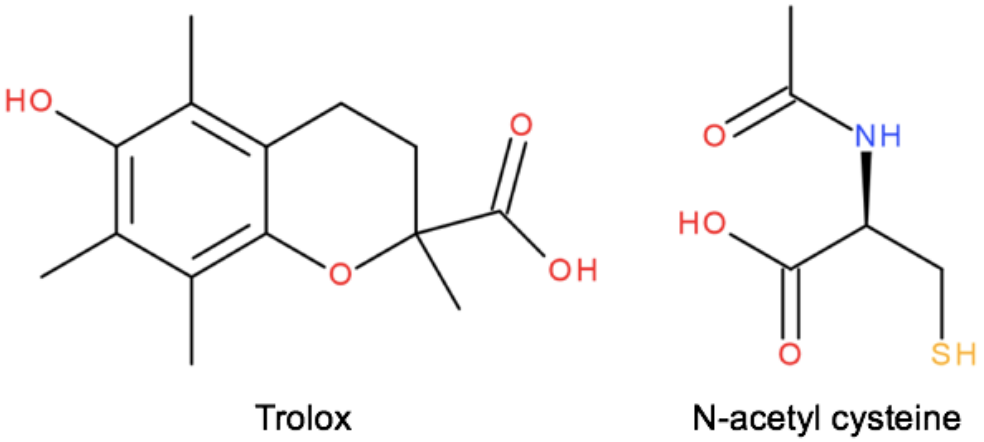

Figure 1.6 Trolox and N-acetyl cysteine are antioxidants that scavenge reactive oxygen species (ROS).

The simplest way to measure the oxidative stress caused by a compound is by conducting a survival assay coupled with a rescue assay. In a survival assay, the survival of a test organism is determined at increasing chemical concentrations. If incubation in an antioxidant (for example, Trolox (6-hydroxy-2,5,7,8-tetramethylchroman-2-carboxylic acid) or N-acetyl cysteine, which are both ROS scavengers [37]) in a subsequent rescue assay increases the organism's survival rate, it can be postulated that oxidative stress contributed to the cause of death.

These assays are complemented by live ROS-staining assays. Since they measure ROS rather than biological macromolecules, ROS-staining assays measure oxidative stress irrespective of the pathway. The production of mitochondrial or cytosolic ROS can be distinguished from one another using fluorescent probes like Mitotracker® Red CM-H_2XRos for mitochondrial ROS and 2',7'-dichlorodihydrofluorescein diacetate (H_2-DCFDA) for cytosolic ROS [38]). These probes function by reacting with ROS,

producing a fluorescent product. For example, as H_2DCFDA enters a cell, it is cleaved by esterases to form a non-fluorescent product, 2',7'-dichlorodihydrofluorescein (H_2-DCF) (Figure 1.7). H_2-DCF reacts with cytosolic ROS to produce 2',7'-dichlorofluorescein (DCF), which fluoresces green (excitation/emission 470/525 nm). The fluorescence is quantified to estimate the ROS produced in changing environmental conditions, such as oxidative distress caused by pollutants.

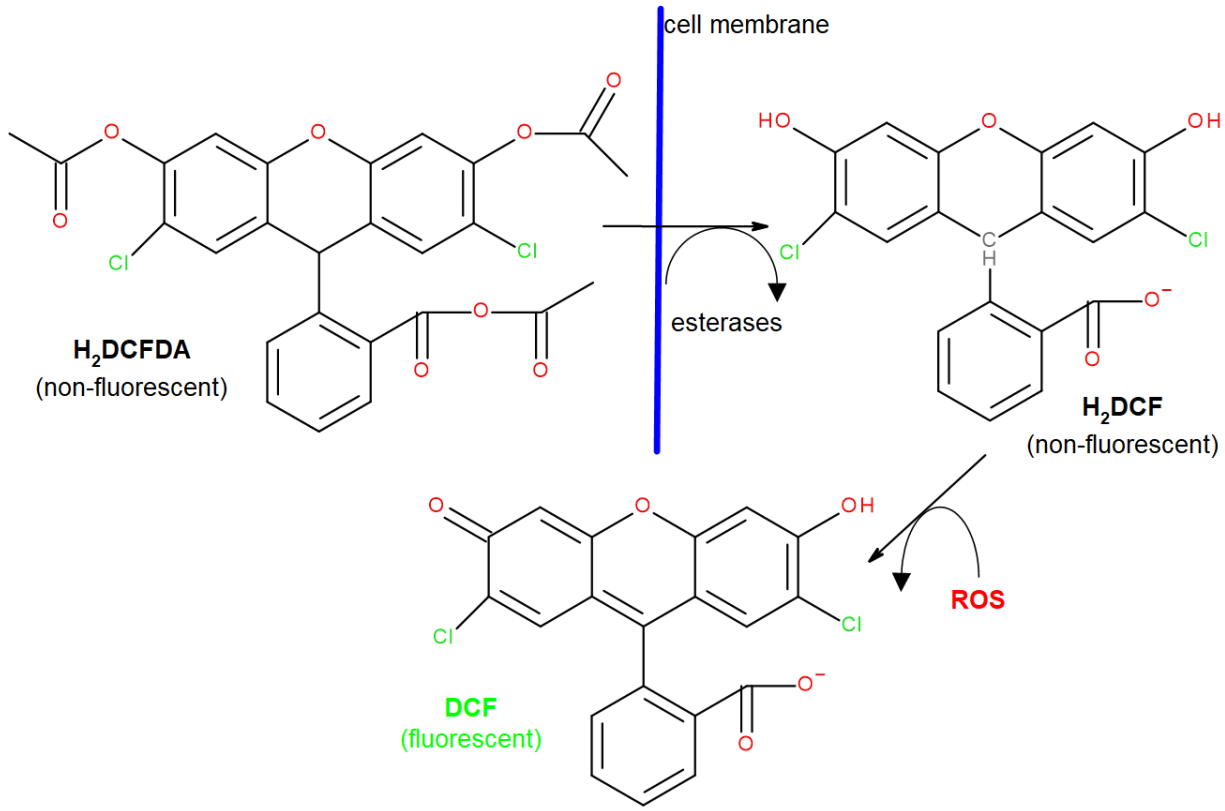

Figure 1.7 2',7'-Dichlorofluorescein (DCF) is used to quantify cytosolic ROS. After H_2-DCFDA is cleaved by cytosolic esterases, the resulting H_2-DCF reacts with ROS to produce DCF, which fluoresces green.

1.3.2 Individual markers

There are also western blot and quantitative polymerase chain reaction (qPCR) approaches for individual or small sets of protein and gene markers, respectively. These markers might include antioxidant enzymes (or their messenger ribonucleic acid (mRNA)

transcripts) that directly detoxify ROS, like SOD and catalase; that scavenge ROS, like heme oxygenase-1 (which catalyzes the degradation of free heme, producing carbon monoxide, iron, and biliverdin); or glutathione metabolizing enzymes like GST (a phase II metabolism enzyme that helps eliminate xenobiotic compounds) [12]. qPCR methods use thermocyclers to amplify the complementary DNA (cDNA) sequences of biomarkers, and then quantify the product mRNA. Western blot (which is used in this thesis) examines specific protein expressions, and requires multiple steps.

Each step in a western blot can be altered to optimize the detection of the chosen analyte. In a typical western blot, proteins are first denatured to have a uniform shape, then separated by molecular weight by sodium dodecyl-sulfate polyacrylamide gel electrophoresis (SDS PAGE). The proteins on the gel are then electroblotted onto a polyvinylidene difluoride (PVDF) membrane. Following a blocking step in either milk or bovine serum albumin (BSA) to reduce non-specific antibody binding, the membrane is incubated in a primary antibody solution that binds to the protein of interest (for example, to the chosen marker for oxidative stress). The membrane is washed, then a second antibody incubation is performed, where the secondary antibody binds to the primary antibody. The membrane is washed again, and the secondary antibody can then be detected in a couple different ways. If the secondary antibody is bound to a fluorophore, it can be detected by fluorescence imaging. If it is bound to the enzyme horseradish peroxidase (HRP), the membrane is incubated in the enzyme's substrate (hydrogen peroxide) and luminol, and the resulting light is detected by enhanced chemiluminescence. The light detected is compared to the total protein blotted onto the membrane to generate a normalized protein signal for each sample.

Unfortunately, there are some difficulties with both methods. With western blot, getting antibodies that bind specifically to the chosen marker is crucial, but these primary antibodies can become quite expensive (hundreds of dollars for small volumes) if the marker is not well-studied or impossible to find if the test organism is obscure. Any time a new marker is chosen, the western blot steps (including gel density, incubation times, and incubation concentrations) need to be optimized to the marker of interest, and this troubleshooting can be very labour-intensive [39]. With qPCR, the greatest expense is the qPCR machine, which can cost thousands of dollars. The supplies are also expensive; they can raise the cost to over 2 dollars per replicate, making qPCR a less attractive method for most labs to pursue. Along with the troubleshooting and high expense involved in western blot and qPCR, respectively, gathering data for individual oxidative stress markers is labour intensive and may not show any critical reactions. In both methods (with maybe only a few markers of oxidative stress being monitored per experiment), it is possible that no change will be noticed between control groups because the pro-oxidant may have no effect on the markers chosen. Therefore, only conducting western blot and qPCR, which detect a limited number of oxidative stress biomarkers, may miss relevant biological changes.

1.3.3 Protein carbonylation

An alternative method for monitoring oxidative stress in proteins is by measuring total protein carbonylation. Carbonyl groups (aldehydes and ketones) can be derivatized with 2,4-dinitrophenylhydrazine (DNPH) to form dinitrophenyl (DNP) groups. After the derivatization, DNP groups can be quantified using anti-DNP antibodies in an OxyBlot (a modified version of a western blot). The resulting blots have multiple bands of varying

molecular weight as the assay is not specific to a certain protein, but rather to carbonyl groups on any protein. Additionally, protein carbonylation can be artificially increased by nucleic acid contamination or the presence of thiol in the lysis buffer [40].

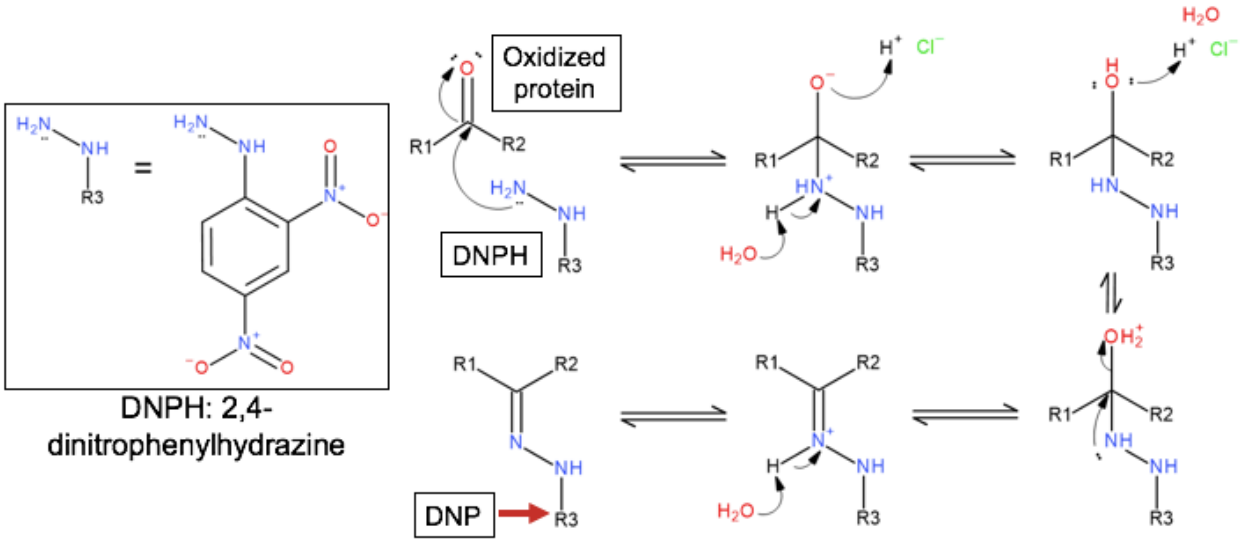

Figure 1.8 2,4-Dinitrophenylhydrazine (DNPH) attacks the ketone and aldehyde groups of oxidized proteins, resulting in the derivatization of proteins with dinitrophenyl (DNP) groups. DNP groups are detectable by western blot.

There is also evidence that the reformulation of OxyBlot kits (from dissolving DNPH in 100% trifluoroacetic acid to dissolving it in hydrochloric acid) has resulted in decreased sensitivity between controls and a lack of reproducibility [41]. Each of these factors may lead to a high background signal, so OxyBlot tests should be conducted alongside other oxidative stress tests.

1.3.4 Proteomics and genomics

Rather than monitoring a single marker at once, multiple DNA and protein markers can be can be analyzed at once using genomics- or proteomics-based approaches. Microarray technology, where the expression of tens of thousands of transcripts are measured at once, allows researchers to study an organism or cell's systemic response

to oxidative stress [42]. Since changes in mRNA transcripts do not necessarily change the phenotypic profile, gene array tests can be strengthened by combining them with proteomics-based analyses, such as liquid chromatography-mass spectrometry (LC-MS)-based proteomics or high-throughput protein microarrays [42, 43]. These methods cast a wide net, but depend on reliable patterns of gene regulation and expression.

1.3.5 Lipid peroxidation

Since lipid peroxidation is independent of gene expression and can occur as soon as ROS are produced, it is a popular biomarker for oxidative stress. The extent of lipid peroxidation is quantified by measuring the generation of lipid peroxidation products, like MDA, 4-HNE, and isoprostanes (iso-Ps), which can be done in many ways [17]. MDA concentrations have often been measured using the colorimetric thiobarbituric acid reacting substances (TBARS) assay, where MDA reacts with thiobarbituric acid to form a pink product that absorbs light at 525 nm, but this reaction is nonspecific and not quantitative [16]. Additionally, the concentration of free MDA and 4-HNE *in vivo* is likely to be low since the aldehydes readily conjugate to biomolecules [44]. 4-HNE can be measured with an immunoassay like western blot or enzyme-linked immunosorbent assay (ELISA), though the antibodies should be raised against 4-HNE-conjugated proteins [44]. Either of these aldehydes can instead be sensitively measured using GC-MS [44]. Iso-Ps can be quantified by LC-MS, along with many other oxylipins, to detect the mounting biological response to oxidative stress [17].

1.4 Oxylipins

ROS produced during oxidative stress target PUFAs associated with membrane phospholipids, creating oxylipins (which include iso-Ps and many other compounds) [45].

Oxylipins are the stable secondary products of lipid peroxidation and metabolites produced through regulated enzymatic action. They comprise a complex class of potent signalling molecules in the modulation of oxidative stress [46]. For these reasons, monitoring global oxylipin production by LC-MS may provide mechanistic information on an organism's oxidative stress response.

1.4.1 Production

In the production of oxylipins, dietary fatty acids (including omega-3s, like docosahexaenoic acid (DHA) and eicosapentaenoic acid (EPA); and omega-6s, like linoleic acid (LA) and arachidonic acid (ARA)) are converted, either by auto-oxidation, or by three major enzyme classes: cytochrome p450s (CYP), lipoxygenases (LOX), and cyclooxygenases (COX). CYPs epoxidize ARA (the most widely distributed PUFA in humans), forming isomers of epoxyeicosatrienoates (EETs) and hydroxyeicosatetraenoates (HETEs) [47, 48]. The EETs are then be hydrolyzed by soluble epoxide hydrolase (sEH) to dihydroxyeicosatrienoates (DHETs) [48]. LOX enzymes hydroxylate arachidonic acid, producing hydroperoxyeicosatetraenoates (HpETEs), which are rapidly reduced to HETEs [49]. Downstream products of these HETEs are leukotrienes [50]. The last enzyme class—the COX pathway—cyclizes and oxidizes free fatty acids, producing oxylipins called prostaglandins (PGs) [51]. The acronyms of oxylipins resulting from alternative PUFAs are listed in Table 1.2.

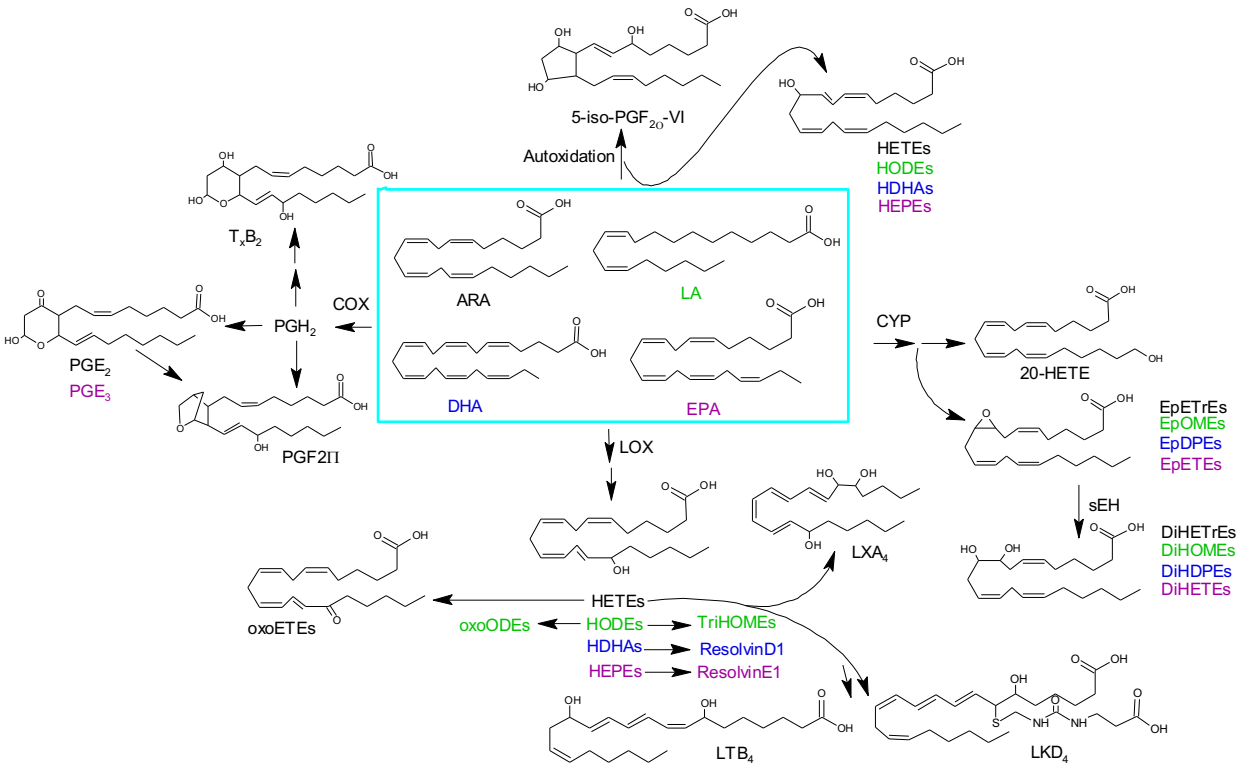

Figure 1.9 PUFAs (ARA, LA, DHA, and EPA) are converted by auto-oxidation and by three major enzyme classes (CYP, LOX, and COX) to potent signalling molecules called oxylipins. These oxylipins are then converted to secondary metabolites (colour-coded based on the starting PUFA) with alternative or more potent biological effects. Figure by Erin Lange of the Rand lab.

Table 1.2 The EETs, DHETs, and HETEs produced during the metabolism of four major PUFAs

Initial PUFA	Corresponding EET	Corresponding DHET	Corresponding HETE
ARA	EpETrE (or EET)	DiHETrE (or DHET)	HETrE (or HETE)
LA	EpOME	DiHOME	HODE
DHA	EpDPE	DiHDPE	HDHA
EPA	EpETE	DiHETE	HEPE

Finally, iso-Ps are the prostaglandin-like products of free radical-mediated auto-oxidation, a process that lacks the stereospecificity of the enzymatic pathways [45, 52]. The oxylipins from each of these pathways are discrete signalling molecules that promote and

maintain inflammatory signalling cascades, demonstrating the impact of oxidative stress on signalling and physiological effects [48]. Figure 1.9 demonstrates the complexity of the pathways, showing how the initial products can be converted to secondary metabolites. The secondary metabolites, which are also oxylipins, have alternative or more potent biological effects [53].

1.4.2 Physiological effects

While oxylipins are the products of PUFA oxidation, different classes of oxylipins have alternative effects on oxidative stress and inflammation. Prostanoids (PGs and iso-Ps) and leukotrienes are generally pro-inflammatory, whereas the EETs from the CYP pathway and other epoxy fatty acids (EpFAs) are generally anti-inflammatory [48]. Many of the oxylipins' effects can be related back to modulating oxidative stress.

Iso-Ps are the product of the nonenzymatic free radical-catalyzed peroxidation of arachidonic acid, and they are considered the best biomarkers for oxidative stress in biological systems [54]. Iso-Ps (especially $PGF_{2\alpha}$–like isoprostanes, like 8-iso-$PGF_{2\alpha}$) are popular biomarkers for many reasons: Iso-P formation is correlated with increased oxidative stress, they can be accurately quantified by LC-MS/MS at picomolar concentrations, they are stable in non-invasive biological samples (for example, in breath and urine), and they are not affected by dietary lipid content [55, 56]. Meanwhile, Iso-Ps are also used as biomarkers for disease states, and may mediate some of the features of those disease states [55].

Other oxylipins—like PGs (which are stereoisomers of Iso-Ps), HETEs, and leukotrienes—are also biomarkers of oxidative stress or inflammation, but they are formed by either the COX and LOX enzyme classes. Pro-inflammatory mediators like

PGE_2 stimulate ROS production, which then stimulates further inflammation, creating a cycle of increasing oxidative stress and inflammation [57]. This cycle can lead to disease states like Creutzfeldt-Jakob disease [58]. In patients with this brain disease, COX-2 enzymes are selectively upregulated in microglial cells (immune cells in the central nervous system) to produce prostaglandin E_2 (PGE_2) and ROS [59, 58]. Regardless of when symptoms of the disease start, patients with lower PGE_2 concentrations have longer survival times, suggesting PGE_2 is a marker for Creutzfeldt-Jakob disease severity [58]. Blocking the production prostaglandins like PGE_2 could therefore have substantial physiological effects.

When PGE_2 production is blocked by COX-2 inhibition, ARA metabolizes through either the LOX or CYP pathways instead, forming oxylipins like HETEs [60]. HETEs increase mitochondrial dysfunction, oxidative stress, and inflammation, resulting in various disease pathologies. When endothelial cells were incubated with 12-HpETE (an ARA metabolite by LOX that rapidly degrades to 12-HETE), the mitochondrial membrane potential was reduced and mitochondrial respiration was impaired [61]. 20-HETE, which is produced by the CYP pathway, induced superoxide production in human umbilical vascular endothelial cells, linking it with an increase in oxidative stress [62]. 20-HETE also activated nuclear factor kappa-light-chain-enhancer of activated B cells (NF-κB), a pro-inflammatory transcription factor [63]. This NF-κB activation resulted in endothelial activation and dysfunction, implicating the oxylipin in pathogenic conditions like atherosclerosis, cardiovascular disease, and hypertension [63]. HETEs produced by both the CYP and LOX enzyme pathways increase stress *in vivo*, but the metabolism of LOX-derived HETEs leads to additional stress-inducing oxylipins called leukotrienes.

Leukotriene A_4 (LTA_4) is produced by the 5-LOX-catalyzed epoxidation of HETEs, and is a precursor to potent pro-inflammatory leukotrienes [64, 65]. LTA_4 is hydrolyzed to the diol leukotriene B_4 (LTB_4), or conjugated with glutathione to form the cysteinyl-leukotrienes: LTC_4, LTD_4, and LTE_4 [64]. LTB_4 is a key mediator in inflammation, as demonstrated in high fat diet mice: the inhibition of their LTB_4 receptor resulted in an anti-inflammatory phenotype [66]. Leukotrienes have also been associated with increased oxidative stress; when LTC_4 is induced by ER stress, the oxylipin mediates ROS accumulation and oxidative DNA damage [67]. Eventually, the downstream action of LTC_4 and its metabolites inflict symptoms of asthma [67]. Given its role in ER and oxidative stress responses, the inhibition of LTC_4 and perhaps other leukotrienes could reduce the pathologies associated with ER stress.

While most products of auto-oxidation and the three enzyme pathways generally increase oxidative stress, their opposing counterparts are the EETs and other EpFAs from the CYP pathway, which are anti-inflammatory and analgesic [48]. These oxylipins have epoxide moieties that do not react with biological nucleophiles (like DNA), but that are quickly hydrolyzed by epoxide hydrolases like sEH [48, 68]. However, the effects of EpFAs have been demonstrated in studies that inhibit sEH and, as a result, build up EpFA stores. For example, sEH inhibition (sEHI) reduced pulmonary fibrosis in mouse models [69]. In rats with PGE_2-induced pain, the combination of sEHI and CYP450 induction had a significant analgesic effect [70]. Though more research should be done, a possible mechanism behind the modulation of pain and inflammation by EpFAs is the attenuation of ER stress, which is implicated in the pathogenesis of many diseases [48, 71]. ER stress is characterized by excessive unfolded proteins in the cell and it is exacerbated by

oxidative stress and mitochondrial dysfunction, both of which are reduced by EpFAs [48, 71, 72, 73].

Since each of the oxylipins mentioned above are created from the same stores of dietary fatty acids (ARA, LA, DHA, and EPA), blocking one of the enzyme pathways will simply shunt the lipids down another metabolic pathway. Depending on which pathways are blocked and which oxylipins are produced when test models are exposed to xenobiotics, oxidative stress may increase or decrease. If many of the potential metabolites are monitored, it is less likely that biological changes will be missed. This approach provides a mechanistic overview of the oxidative stress response while also offering an expression-independent measurement of enzyme regulation. For these reasons, it is important to monitor the metabolites of auto-oxidation and each of the three enzyme branches.

1.5 *Caenorhabditis elegans* as a model organism

Each of the oxidative stress testing methods above can be completed using *Caenorhabditis elegans*—a free-living roundworm (nematode)—as a model. *C. elegans* is a simple, small (1 mm), and amenable model organism [74]. It has a far-ranging habitat where it lives and crawls through soil, but it is also able to grow by swimming in solution. It can survive axenically, but it will grow more quickly if it feeds on bacteria like *Escherichia coli* OP50 [75]. Most worms are hermaphroditic (XX) and can self-fertilize, though 0.1% of worms are male (XO) through spontaneous mutations [76]. Although *C. elegans* is a tiny and simple model organism, it has many advantages: it is a low-cost whole organism, it has a short life cycle and a large brood size, it is transparent, there is gene homology with toxicity pathways in humans, and there is a large library of transgenic nematodes.

With all its benefits, *C. elegans* is a powerful model for oxidative stress, making it among the most-studied model organisms, like the fruit fly (*Drosophila melanogaster*) and zebrafish (*Danio rerio*).

There are many reasons for *C. elegans*' popularity in research, starting with its low cost. Many whole organisms used in toxicity tests are mammals like rats and mice. These models are expensive, costing thousands to acquire, house, and feed. In contrast, *C. elegans* mutant strains cost up to $100 to acquire and they feed off *E. coli*, which is cheap to grow with commonly-found lab materials.

Thousands of worms can be propagated within a week of acquiring a new mutant strain. *C. elegans* become fertile after 3.5 days (or less, if they're grown at warmer temperatures), and then each worm lays about 250 eggs within several days [74]. Its short generation time makes reproductive toxicity studies more accessible, and its short generation time and lifespan (about 20 days) make *C. elegans* a good model for measuring the development of toxicity over time [74]. The volume of worms that can be assayed in such a short time allows for statistical power that is hard to achieve in higher model organisms.

Typically, experiments with comparable statistical power use cell lines, but using a whole organism allows researchers to monitor a systemic response to oxidative stress. *C. elegans* does not share all the same organs as a human, though it has a far more complex anatomy than mammalian cells; as shown in Figure 1.10, hermaphroditic worms have a thick cuticle and underlying epithelium, a pharynx, intestines, an excretory system, neurons, muscles, and gonads [76]. Also, since it is a whole organism, *C. elegans* is more

likely to express oxidative stress enzymes and enzymes that bioactivate pollutants, avoiding some of the false negatives that would result from only using cell cultures.

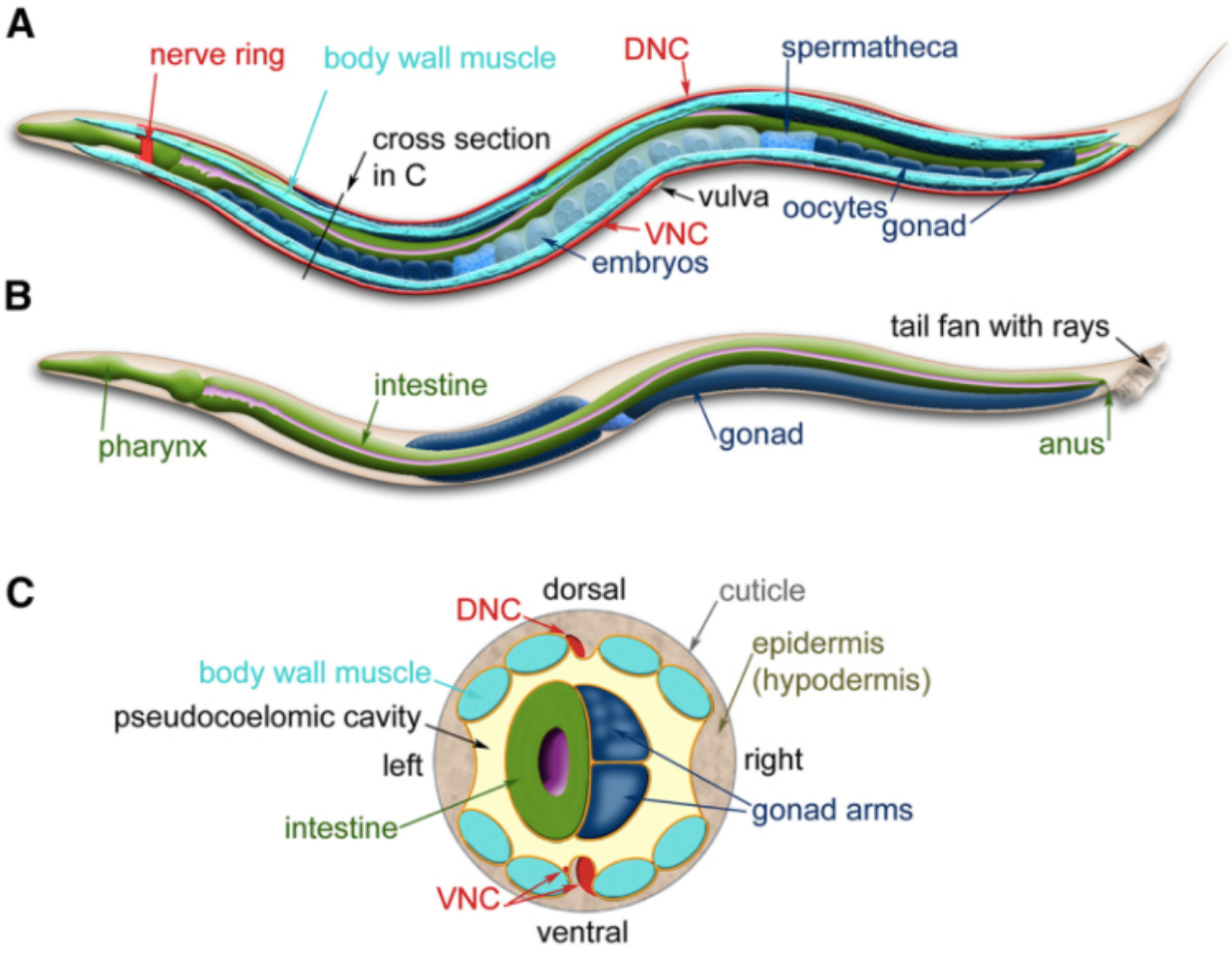

Figure 1.10 The anatomy of hermaphrodite (A) and male (B) *C. elegans*. (A) The dorsal nerve cord (DNC) and ventral nerve cord (VNC) run along the body, starting at the nerve ring at the animal's anterior region. There are four muscle quadrants (as shown in cross section C), with only two shown in A and B. (B) The adult male structure has the nervous system and muscles hidden, displaying the pharynx, intestines, and anus instead. (C) This cross-section shows the intestine and gonads in the pseudocoelomic cavity, and the muscles surrounded by the epidermis and cuticle [77].

However, higher model organisms have more in common with humans than *C. elegans*. About 65% of human genes have homologs in *C. elegans*, whereas the homology between humans and mice is 90% [78, 79]. Many toxic response pathways are conserved, but because *C. elegans* and humans have different toxicokinetic pathways,

they may not always metabolize the same compounds or produce the same metabolites. Their metabolic differences can begin to be addressed by genetically modifying *C. elegans* to express human enzymes, like mtCYP2E1 and erCYP2E1. These mutants already exist, as do thousands of others. There are over 3,000 mutant strains of *C. elegans* that compensate for some of the differences between them and humans [80].

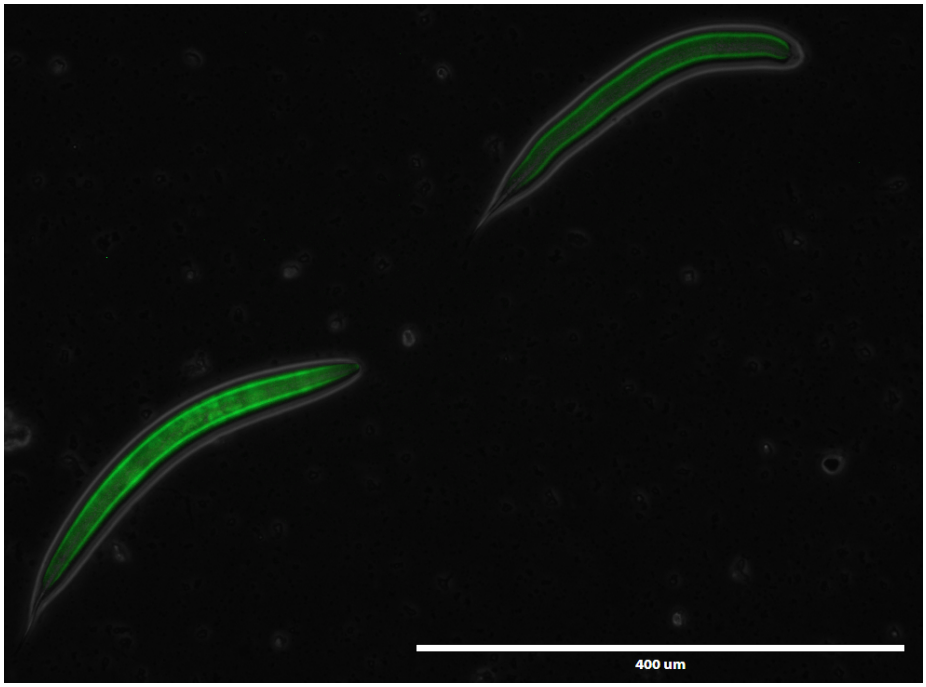

Figure 1.11 Larval stage 4 (L4) erCYP2E1 worms were incubated in 270 mM paraquat, then in 50 μM H_2-DCFDA (an indicator for ROS that, after reacting with ROS, fluoresces green).

One notable difference between the two species—a very advantageous one for *C. elegans* research—is that *C. elegans* is transparent. This unique feature means *C. elegans* can be used in fluorescent reporter assays, where the worms are modified to express a fluorescent protein, like green fluorescent protein (GFP). The expression of GFP is then correlated to the expression of a gene of interest. There are even fluorescent assays that can be used with wild-type worms; fluorescent dyes can be used to quantify compounds like ROS, as shown in Figure 1.11. Combining these assays, analyzing the

fluorescence emitted from nematodes can allow for both the quantification and localization of proteins and ROS within the organism.

1.6 Project aim

The aim of this project was to develop and validate the *C. elegans* model as an appropriate organism to examine oxidative stress upon exposure to environmental contaminants. Two contaminants were used: paraquat, as a positive control to assess oxidative stress; and styrene, to assess differences in ER- and mitochondrial-localized CYP2E1 activation and associated stress. To do this, traditional oxidative stress testing was conducted alongside global oxylipin monitoring. In the future, these data will help clarify which oxylipin-signalling pathways influence the oxidative stress response in the mitochondria and the ER.

2.0 Materials and methods

The sources of the materials involved used in experiments described in this thesis are described below, and their uses are explained in more detail in the following chapters.

2.1 Materials

Wild-type (N2), mtCYP2E1, and erCYP2E1 *C. elegans* strains, as well as *E. coli* OP50, were generously obtained from Dr. Jessica H. Hartman (Medical University of South Carolina, Charleston, SC, USA). Antibodies—Recombinant Anti-superoxide dismutase 2 (SOD2)/MnSOD antibody (ab68155) and Goat Anti-Rabbit immunoglobulin G (IgG) (H + L)-HRP Conjugate (1706515)—were purchased from Abcam (Cambridge, MA, USA) and Bio-Rad (Hercules, CA, USA), respectively. Acetic acid (≥ 99.7%), hydrochloric acid (HCl) (36.5-38%), isopropanol (≥ 99.5%), and methanol (≥ 99.8%) were

purchased from Anachemia (Mississauga, ON, Canada). Bacto™ Tryptone and Bacto™ Yeast Extract were purchased from BD Biosciences Advanced Processing (Miami, FL, USA). 30% Acrylamide/Bis Solution 37.5:1 (99.9%), Clarity Western Peroxide Reagent, Clarity Western Luminol/Enhancer Reagent, SYPRO® Ruby Protein Blot Stain, and N,N,N',N'-Tetramethylethylenediamine (TEMED) were purchased from Bio-Rad (Hercules, CA, USA). Agar, 2,2',2'',2'''-(ethane-1,2-diyldinitrilo)tetraacetic acid (EDTA) (> 99.5%), EDTA (disodium salt, dihydrate) (≥ 99.5%), glycerol (≥ 99%), glycine (≥ 99%), magnesium sulfate ($MgSO_4$) (≥ 99%), potassium hydrogen phosphate (K_2HPO_4) (≥ 99.5%), potassium dihydrogen phosphate (KH_2PO_4) (≥ 99.5%), sodium chloride (NaCl) (≥ 99%), sodium dodecyl sulfate (SDS) (≥ 99%), disodium hydrogen phosphate (Na_2HPO_4) (> 99%), Tris (≥ 99.9%), and Tris-HCl (≥ 99%) were obtained from BioShop Canada (Burlington, ON, Canada). N-acetyl cysteine (≥ 95%), Trolox (≥ 98%), and PUFA and oxylipin standards (≥ 99%) were purchased from Cayman Chemical (Ann Arbor, MI, USA). Ethanol (95%) was obtained from Commercial Alcohols (Brampton, ON, Canada). HPLC-grade ethyl acetate (99.9%) was purchased from Caledon Laboratory Chemicals (Georgetown, ON, Canada). Ammonium persulfate (APS) (≥ 98.0%), calcium chloride dihydrate ($CaCl_2$•2 H_2O) (99-105%), Coomassie Brilliant Blue R-250, dithiothreitol (DTT) (≥ 99.0%), formic acid for mass spectrometry (≥ 97.5%), levamisole hydrochloride (> 99%), and peptone were purchased from Fisher Scientific (Fair Lawn, NJ, USA). LC-MS-grade methanol (>99.9%) was purchased from Honeywell (Muskegon, MI, USA). Lavo '12' Bleach (10.3%) was purchased from LAVO (Montreal, QC, Canada) and skim milk powder was obtained from Loblaws Inc. (Toronto, ON, Canada). 2',7'-Dichlorodihydrofluorescein diacetate (H_2-DCFDA) (≥ 95%), 2-mercaptoethanol (99%),

bromophenol blue, butylated hydroxytoluene (BHT) (≥ 99%), copper (II) sulfate ($CuSO_4$) (≥ 99%), HPLC-grade methanol (≥ 99.9%), iron (II) sulfate heptahydrate ($FeSO_4$•7 H_2O) (≥ 99%), manganese (II) chloride ($MnCl_2$) (98%), methyl viologen dichloride hydrate (paraquat dichloride) (98%), sodium azide (NaN_3) (≥ 99.5%), sodium hydroxide (NaOH) (≥ 99.0%), styrene (≥ 98.0%), tri-potassium citrate monohydrate (≥ 99%), TWEEN® 20 (≥ 40.0%), and zinc sulfate heptahydrate ($ZnSO_4$•7 H_2O) (>99%) were purchased from Millipore Sigma (St. Louis, MO, USA). PageRuler™ Prestained Protein Ladder (26616) was obtained from Thermo Scientific (Rockford, IL, USA). Acetonitrile Omnisolv® LC-MS (≥ 99.9%), cholesterol (95%), citric acid monohydrate (99-102%), and dimethyl sulfoxide (DMSO) (≥ 99.0%) were purchased from VWR (Mississauga, ON, Canada). Propane was obtained from Worthington Cylinder Corporation (Columbus, OH, USA).

There were a few kits used to conduct the experiments in this thesis. The 4-HNE ELISA Kit was purchased from Elabscience (Wuhan, Hubei, China), and the BCA (bicinchoninic acid) Protein Assay Kit as well as the BSA Standards used in these two assays were purchased from Thermo Scientific (Rockford, IL, USA). The OxyBlot Protein Oxidation Detection Kit was purchased from EMD Millipore Corporation (Billerica, MA, USA).

2.2 *Caenorhabditis elegans* maintenance

Three *C. elegans* strains—wild-type, endoplasmic reticulum CYP2E1 (erCYP2E1), and mitochondrial CYP2E1 (mtCYP2E1) worms—were cultured according to the protocol adapted from Stiernagle 2006 [80].

2.2.1 Preparing *Escherichia coli* OP50

C. elegans were grown monoxenically with *E. coli* strain OP50 as a food source. *E. coli* OP50 colonies were streaked on a plate containing lysogeny broth (LB) agar (10 g Bacto™ Tryptone, 5 g Bacto™ Yeast Extract, 5 g NaCl, and 15 g agar topped up to 1 L with distilled water (dH_2O), the pH was set to 7.5, and then the solution was autoclaved in a Model 522LS Gravity Steam Sterilizer (Getinge, Gothenburg, VG and BO, Sweden) and poured into petri dishes, with any unstreaked dishes stored at 4 °C until future use). The plate was sealed then incubated in a MaxQ 5000 Floor-Model Shaker (Thermo Scientific, Rockford, IL, USA) for 18 hours at 37 °C. All 37 °C incubation steps occurred in this incubator, whereas all the 18-22 °C incubations occurred in a Fisherbrand Mini Low Temperature Refrigerated Incubator (also from Thermo Scientific) unless otherwise specified.

Using gloves dipped in 70% ethanol, a sterile pipette tip was used to scratch an isolated bacterial colony. The pipette tip was then placed in a 50 mL Falcon tube containing about 30 mL of LB (10 g Bacto™ Tryptone, 5 g Bacto™ Yeast Extract, and 5 g NaCl topped up to 1 L with dH_2O, the pH was set to 7.0, and then the solution was autoclaved). The tubes were shaken for 18 hours at 37 °C, then stored at 4 °C and used as a bacterial food source (called OP50) for *C. elegans* for a few months.

To prepare *E. coli* for nematode growth in liquid culture, the isolated bacterial colonies were placed in higher volumes of LB (1 L per 125 mL of worms grown) and grown overnight. The pellet was isolated by centrifugation at 3000 x g for 4 minutes.

2.2.2 Preparing Nematode Growth Medium plates

A Nematode Growth Medium (NGM)—made of 3 g NaCl, 2.5 g peptone, 17 g agar and 975 mL of dH_2O—was autoclaved and then cooled to 55 °C in a Precision Circulating Water Bath (Thermo Scientific, Rockford, IL, USA) for 15 minutes. Potassium phosphate pH 6.0 buffer (25 mL, 1 M) (108.3 g KH_2PO_4, 35.6 g K_2HPO_4, topped up to 1 L with dH_2O, and autoclaved), and 1 mL each of 1 M $CaCl_2$•2 H_2O, 1 M $MgSO_4$, and 5 mg/mL cholesterol in ethanol, were added to the solution. The medium was poured into multiple large (100x15 mm) petri dishes. The plates were left to dry over a couple days, then were stored at room temperature in a clean plastic container to avoid further drying.

Just before transferring *C. elegans* to the NGM agar plates, 100 µL of OP50 was added to the plates (this process is called “seeding”). A bent Pasteur pipette was sterilized and used to spread the OP50 evenly around the whole plate, creating a bacterial lawn.

2.2.3 Culturing *C. elegans*

The three *C. elegans* strains were received and transferred to seeded NGM plates, taking care not to combine any of the strains.

Transferring worms to freshly-seeded NGM plates happened at least once every week, and could be done by either picking a single worm (“picking”) or cutting out an agar chunk of a plate with a large amount of age-mixed worms (“chunking”). Both methods were completed under sterile conditions (with tools dipped in ethanol and flamed).

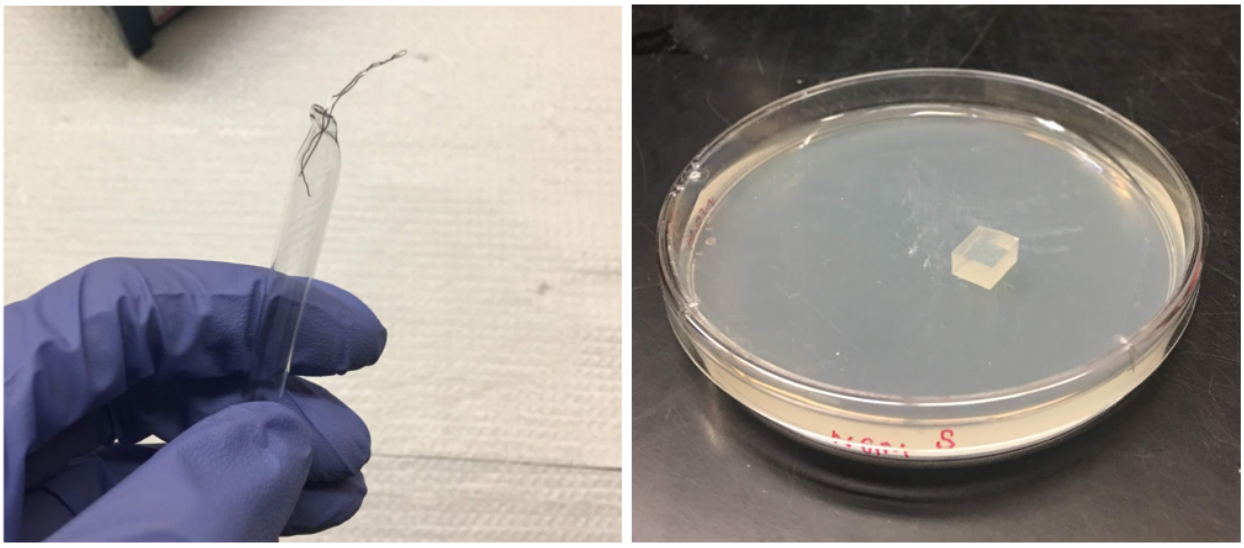

Figure 2.1 On the left, a worm picker made of platinum wire and a Pasteur pipette. On the right, nematodes are transferred to a new agar plate by "chunking" pieces of the NGM agar.

Picking was completed using a worm picker (a 32-gauge platinum wire—with its end bent—attached to a melted Pasteur pipette tip). For chunking, a piece of the old agar plate was cut using a scalpel, then it was transferred to a new, seeded plate.

2.2.4 *C. elegans* growth on agar plates and in liquid media

Since small temperature changes affect *C. elegans* growth rates, *C. elegans* stocks on agar plates were maintained between 18-22 °C in an incubator, depending on the timing of experiments.

To prepare larger quantities of worms, *C. elegans* were cultured in liquid media called S Medium. S Medium was prepared under sterile conditions with 1 L S Basal (5.85 g NaCl, 1 g K_2HPO_4, 6 g KH_2PO_4, 1 mL cholesterol (5 mg/mL in ethanol), topped up to 1 L with dH_2O, and autoclaved), 10 mL 1 M potassium citrate pH 6.0 (20 g citric acid monohydrate, 293.5 g tri-potassium citrate monohydrate, topped up to 1 L with dH_2O, and autoclaved), 10 mL trace metals solution (1.86 g EDTA (disodium salt, dihydrate), 0.69 g

$FeSO_4$•7 H_2O, 0.13 g $MnCl_2$, 0.29 g $ZnSO_4$•7 H_2O, 0.016 g $CuSO_4$, topped up to 1 L with dH_2O, autoclaved, and stored in the dark), 3 mL 1 M $CaCl_2$•2 H_2O, and 3 mL 1 M $MgSO_4$.

S Medium (125 mL) and the pellet of a 1 L solution of *E. coli* OP50 were added to a sterile 500 mL flask. Freshly-starved *C. elegans* were washed off 4 large plates into the flask, using 5 mL of S Medium per plate. The worm flasks were vigorously shaken at room temperature on a Standard Orbital Shaker (Model 3500) (VWR, Mississauga, ON, Canada). Additional concentrated *E. coli* was added if the solution was no longer cloudy. Once a droplet of the worm solution contained many animals, the worms were ready to be harvested (after about 4 days of shaking).

2.2.5 *C. elegans* long-term storage

When stocks were not needed for experiments, they were frozen in Soft Agar Freezing Solution (0.58 g NaCl, 0.68 g KH_2PO_4, 30 g glycerol, 0.56 mL 1 M NaOH, 0.4 g agar, topped up to 100 mL with dH_2O, and autoclaved, then microwaved if it solidified). Three large NGM plates (full of freshly starved animals, explained in section 2.2.6) were washed with 0.6 mL S Buffer (129 mL 0.05 M KH_2PO_4, 871 mL 0.05 M KH_2PO_4, and 5.85 g NaCl, and autoclaved). The liquid was collected in a covered, sterile test tube and placed on ice for 15 minutes. An equal volume of Soft Agar Freezing Solution was added to the test tube and mixed well, then 1 mL aliquots of the final solution were added to cryotubes. The tubes were stored in a Styrofoam container overnight at -80 °C, then removed from the container and transferred to their permanent location in freezer boxes (also at -80 °C).

To recover frozen stocks, scoops comprising about a quarter to a third of the frozen solution were removed using a sterile spatula, then added to a seeded NGM plate. The still-frozen tube could then be returned to storage at -80 °C.

2.2.6 Obtaining clean or synchronous *C. elegans* stocks

Contamination from bacteria, yeast, and mold could occur regularly if cleaning precautions were not followed. These precautions included sterilizing pipette tips and solutions; preparing sterile aliquots of solutions in a 1300 Series A2 Biological Safety Cabinet (Thermo Scientific, Rockford, IL, USA); cleaning counters with 70% ethanol prior to pouring LB agar or NGM plates; allowing the plates to dry prior to being stored; and scrubbing any contaminated plastic surfaces (such as plate containers) with soap then water, then soaking the plastic in 1:9 bleach to water for 30 minutes.

Seeded NGM plates were especially susceptible to fungal and bacterial contamination. If NGM plates containing worms became contaminated, there were a couple of ways to avoid spreading the contamination to new plates. The first was by serial transferring, and the second was by bleaching.

Serial transferring of worm plates eliminated contamination if it was completed quickly enough and if the contamination was not extensive. Once the contaminated chunk was placed on a new plate, the next chunk transfer had to be completed after the worms have crawled away from the chunk, but before the bacterial or fungal growth had spread to the rest of the plate. The ideal time to chunk again was within a day and this process sometimes needed to be repeated a couple times.

A more effective way of cleaning contaminated plates was by bleaching because it killed the bacterial and fungal contamination on the first try so it did not need to be

repeated. The process started with washing well-fed and full worm plates with sterile M9 (3 g KH_2PO_4, 6 g Na_2HPO_4, 5 g NaCl, 1 ml 1 M $MgSO_4$, topped up to 1 L with dH_2O, and autoclaved), and the liquid (2.1 mL per large plate) containing the worms was collected in a Falcon tube. If the worms were grown in liquid media, the worms were transferred to Falcon tubes and spun down at 1300 x g for 3 minutes (all spins in this section are 3 minutes at 1300 x g in an LSE™ Compact Centrifuge from Corning (Corning, NY, USA)) and the supernatant was discarded. At least 4 mL of a fresh bleach mixture (2.35 mL dH_2O, 1.25 mL 2 M NaOH, and 0.4 mL 12% bleach) were added to the pellet and the solution was vortexed for 9 minutes. This solution contained eggs only since the bleaching conditions dissolved the larval and adult worms. After vortexing, the tube was filled with M9 to dilute the bleach. The resulting embryos were spun down, the supernatant was discarded, and the tube was filled with more M9. The spin and discard steps were repeated 2 more times, but on the second time, some supernatant was left in the tube to be vortexed with the pellet. The resulting solution containing eggs was then dripped onto seeded NGM plates (250 µL onto a fresh plate per 4 large plates bleached, or if the worms had been grown in liquid culture, the egg solution was aspirated down to 5 mL (per 125 mL of worms grown), and added in 250 µL aliquots to fresh plates).

This same bleaching procedure was also used to create a synchronized plate of worms, in which all the worms were at the same life cycle stage. At the end of the procedure, the eggs were placed on an unseeded plate rather than a seeded plate. The worms entered the first larval stage (L1) within 24 hours, but were stalled at this stage due to the lack of a food source. *E. coli* OP50 could then be introduced to the plate, allowing the L1s to proceed to the second larval stage simultaneously.

2.3 Exposure to test substances

Worms were exposed to either of two environmental contaminants: styrene or paraquat dichloride (from now on, referred to as paraquat) dissolved in M9 buffer. The negative control groups were only exposed to M9.

2.3.1 Growing and synchronizing worms

To propagate enough worms for the toxicant exposure tests, many plates of each of the three *C. elegans* strains were chunked. The number of large plates grown per strain, per control group, varied between 4 and 40, though growing more plates resulted in higher volumes of protein for downstream testing (32 plates were ideal for these tests). A few days after chunking, there were enough worms on each plate to synchronize the age groups (following the protocol in 2.2.6). However, more biomass was required for oxylipin samples, so the worms synchronized for those tests were cultured in liquid media (following protocol 2.2.4) prior to bleaching.

2.3.2 Test reagent exposure parameters

For every 4 worm plates bleached, one unseeded NGM plate was prepared with 250 µL of eggs. For example, if 32 plates were bleached, there would be 8 final plates, each with 250 µL of eggs. For tests requiring more biological mass, like analysis by mass spectrometry, the worms were grown in 125 mL of liquid culture (see protocol 2.2.4) rather than on agar plates. Once the three strains were bleached and centrifuged, the resulting pellets (suspended in 5 mL M9 per 125 mL worms grown) were divided into 250 µL aliquots, which were deposited on unseeded NGM plates. OP50 (100 µL) was added directly to the plates the next day (after the eggs had hatched). The worms were incubated for 28 hours at 22 °C, allowing them to grow to larval stage 4 (L4).

The nematodes remained on agar plates during the styrene exposure tests. The test solutions (500 µL of either M9 or 500-5000 µM styrene in M9) were added directly to the hatched worm plates. The plates were then sealed with Parafilm and stored at room temperature. The same volume of solution was added to each plate every 12 hours, sealing the plates each time, to a total of 4 additions of 500 µL solution added over 48 hours.

For the paraquat exposure tests, the nematodes were drawn off the agar plates and were incubated in liquid test solutions. There were two different types of paraquat exposure tests. The first ended in the analysis of whole worms for either a survival assay, a rescue assay, or a fluorescence assay (each explained further in section 2.8). The second set of exposure tests ended in the homogenization of the worms for western blot, ELISA, or ultra-performance liquid chromatography with tandem mass spectrometry (UPLC-MS/MS).

For the paraquat test ending in homogenization, the worms were washed off the plates with 3.65 mL of M9 per plate then centrifuged for 10 minutes at 1150 x g in an LSE™ Compact Centrifuge. The supernatant was aspirated, then the pellet was aliquoted into separate 2 mL centrifuge tubes for each test concentration. The pellets in each tube were approximately 250 µL. Varying volumes of 0.5-2 M paraquat in M9 were added to the positive control samples to obtain a final concentration of 30 and 150 mM paraquat in the pellets, and a similar volume of M9 was added to the negative control sample. The centrifuge tubes containing the worms in 0, 30, and 150 mM paraquat were placed on an MTS shaker and shaken for 2.5 hours at room temperature.

2.3.3 Ending the exposure test

At the end of the 48-hour styrene test, sterile M9 was added to each plate, and the liquid from each plate was collected in 2 mL centrifuge tubes. More M9 was added to the plates until the cryotubes were full. The tubes were spun down for 10 minutes at 10000 x g and 4 °C on a Centrifuge 5424 R (Eppendorf, Hamburg, HH, Germany) (this centrifuge was used for the rest of the steps in this protocol), and the supernatants were discarded. The pellets of the same strain and control group were combined into 1 2-mL cryotube and the spin was repeated.

For the paraquat tests ending in homogenization, the centrifuge tubes were spun down at 6000 x g and 4 °C for 10 minutes, then their pellets were transferred to cryotubes containing ceramic beads (either using a Hard Tissue Homogenizing Precellys CK28 Lysing Kit (Bertin Instruments, Montigny-le-Bretonneux, IDF, France) or a CKMix – 2 mL Tissue Homogenizing Kit (ESBE Scientific, Markham, ON, Canada)). The pellets were spun down again and completely aspirated (except for paraquat samples to be analyzed by western blot, which were aspirated until there was about 200 µL of liquid above the pellet). The pellet of samples meant to be analyzed on UPLC-MS/MS (for oxylipins) was reconstituted in 400 µL ice-cold HPLC-grade methanol with 0.1% acetic acid and 0.1% BHT before transfer to a CKMix – 2 mL Tissue Homogenizing Kit cryotube.

The final pellets were either homogenized immediately (following protocol 2.4) or stored overnight at -20 °C before homogenization.

2.4 *C. elegans* homogenization

Western blot, ELISA, and LC-MS tests each required homogenized *C. elegans* samples. To begin the homogenization, *C. elegans* pellets from section 2.3.3 were

thawed and homogenized using a Bertin Minilys Personal Homogenizer (Bertin Instruments, Montigny-le-Bretonneux, IDF, France). To reduce temperature effects (the excess heat produced in samples during homogenization), the glass grinding beads (Spiral Pestle Grinding Beads from BioSpec Products, Bartlesville, OK, USA) and the removable parts of the homogenizer were stored at -20 °C prior to use.

To begin, 10 µL of an antioxidant solution (0.2 mg/mL BHT and 1 mg/mL EDTA) were added to the cryotubes containing the thawed worm pellets. Some additional components were added to the styrene samples: 0.20-0.26 g of cold, glass grinding beads, and 50-400 µL of either lysis buffer (50 mM Tris-HCl, 2% SDS, and 2% 2-mercaptoethanol) or M9. Surrogate solutions (2.5 µL each of oxylipin and PUFA internal standards) were added to the oxylipin samples (in other words, the standards were only added to samples processed for UPLC-MS/MS analysis). The tubes were homogenized for 20 seconds on the highest homogenization setting, then rested on ice for 30 seconds. These steps were repeated five more times, then the samples were centrifuged for 10 minutes at 13200 x g and 4 °C. The supernatant was aspirated and set aside into a fresh tube. The pellet for UPLC-MS/MS testing was washed with an additional 100 µL of ice-cold HPLC-grade methanol with 0.1% acetic acid and 0.1% BHT, lysed three more times, and spun down again. The pellets of all other samples were spun down again (with no additional buffer). The second supernatant for each test was combined with the first. The methanol-based supernatants were purged of oxygen using an OA-SYS^{TM} Heating System (Organomation, Berlin, MA, USA), and then stored at -20 °C until extraction (see protocol 2.9). The protein in M9- and lysis buffer-based supernatants was quantified, then both the pellets and supernatants were stored at -20 °C.

2.5 Protein quantification

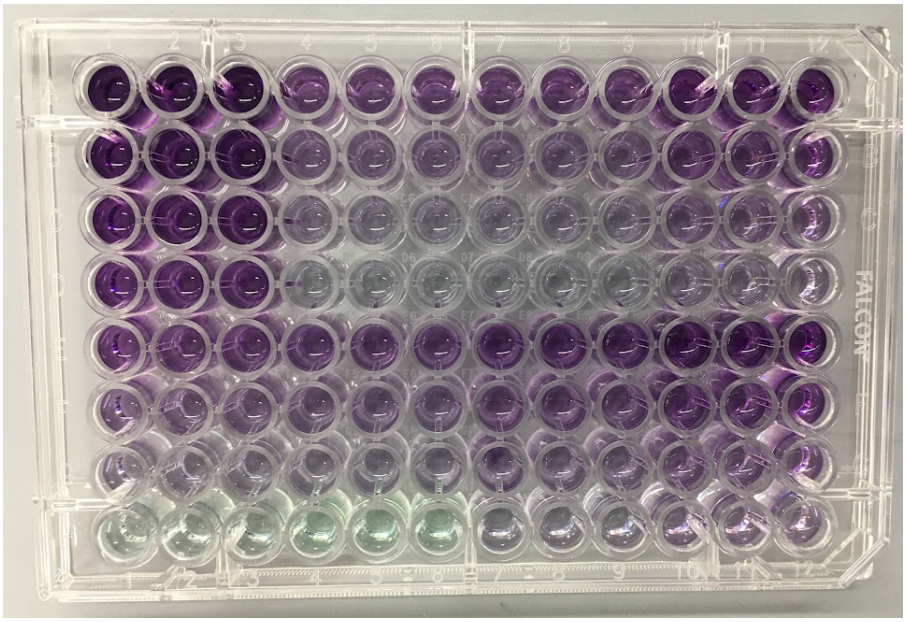

Figure 2.2 Bovine serum albumin (BSA) standards and lysed *C. elegans* samples stained purple following an incubation in bicinchoninic acid assay reagents.

The protein concentration of the M9- or lysis buffer-based supernatants from section 2.4 was measured using a Pierce BCA Protein Assay Kit and BSA standards. The standards and samples were diluted with M9 (with the standards diluted to 0, 25, 125, 250, 500, 750, 1000, 1500, and 2000 mg/mL; and the samples diluted by 2, 4, and 8X), then 25 µL of each dilution were added in triplicate to a 96-well microplate. Working reagent (200 µL) (50 parts reagent A to 1 part reagent B) was added to standard and sample wells. The microplate was shaken for 30 seconds, then incubated at 37 °C for 30 minutes. The absorbance of the resulting BCA/copper complexes was measured at 562 nm using a SpectraMax 340 Microplate Spectrophotometer (Molecular Devices, Sunnyvale, CA, USA).

2.6 Protein assays

Two types of blots were performed: a protein oxidation blot, using an OxyBlot Protein Oxidation Detection Kit; and a traditional western blot assaying for superoxide dismutase 2 (SOD-2). There is considerable overlap between the two methods with some key distinctions, particularly in sample preparation. Both samples, though, were thoroughly washed to remove *E. coli* (since bacterial proteins may bind with the antibodies used in these experiments) [39].

2.6.1 OxyBlot sample preparation

Prior to being run on the gel, samples prepared for the OxyBlot assay first needed to be derivatized with DNPH. About 4 µg of the quantified protein sample was added to each of two 1.5-2.0 mL centrifuge tubes (one tube was the derivatized solution and one was the negative control). The volume of the sample varied depending on its concentration. Assume 4 µL of sample were added to the tubes; however, if this volume were to change, the volume of other reagents was also adjusted.

Each 4 µL aliquot of protein was denatured with an equal volume of 12% SDS. 8 µL of the 1X DNPH solution were added to the derivatized solution and 8 µL of the 1X Derivatization-Control Solution were added to the negative control. Both tubes were incubated at room temperature for 15 minutes, then the reactions were stopped upon the addition of 6 µL of the Neutralization Solution. 2-mercaptoethanol (1.1 µL) was added to each sample for a final concentration of 5.5%. The resulting solution was ready to be loaded on the gel without the addition of a loading buffer.

2.6.2 SOD-2 blot sample preparation

Immediately following the protein quantification step (protocol 2.5), 5X loading buffer (3 mL 20% SDS and 3.75 mL 1 M Tris-HCl, with the pH set to 6.8, then the addition of 9 mg bromophenol blue, 1.16 g DTT, and 4.5 mL glycerol, topped up to 15 mL) was added to the protein samples for a final dilution of 1X. The samples were heated for 3 minutes at 95 °C on a Standard Heatblock (Troemner, Thorofare, NJ, USA), then stored at -20 °C.

2.6.3 Gel electrophoresis

SDS PAGE was performed in a Bio-Rad Mini PROTEAN Tetra Cell (Bio-Rad, Hercules, CA, USA) with a 4% stacking gel (6.1 mL dH_2O, 1.3 mL 30% Bio-Rad acrylamide/bis, 2.5 mL Tris-HCl (0.5 M, pH 6.8), 100 µL 10% SDS, 10 µL TEMED, and 100 µL 10% APS), and a 10% resolving gel (4.1 mL dH_2O, 3.3 mL 30% 37.5:1 Bio-Rad acrylamide/bis, 2.5 mL Tris-HCl (1.5 M, pH 8.8), 100 µL 10% SDS, 10 µL TEMED, and 32 µL 10% APS) for the OxyBlot samples or a 15% resolving gel (2.4 mL dH_2O, 5 mL 30% 37.5:1 Bio-Rad acrylamide/bis, 2.5 mL Tris-HCl (1.5 M, pH 8.8), 100 µL 10% SDS, 10 µL TEMED, and 100 µL APS) for the SOD-2 samples. Protein samples were added to each well for the OxyBlot (4 µg) and SOD-2 (20 µg) gels. A standard Tris/glycine running buffer was used (3.03 g Tris, 14.4 g glycine, and 10.0 g SDS topped up to 1 L with dH_2O). The electrophoresis was performed for about 50 minutes at constant voltage (200 V).

2.6.4 Protein transfer

The transfer from the gel to a PVDF membrane was completed in an XCell II Blot Module (Invitrogen, Waltham, MA, USA) in transfer buffer (3.04 g Tris base, 14.42 g

glycine, 1.00 g SDS, 200 mL methanol, topped up to 1 L with dH_2O, and kept at 4 °C prior to use) at a constant voltage (25 V), submerged in ice, for 1.5 hours.

2.6.5 Total protein stain

The total protein on the PVDF membrane was quantified using SYPRO® Ruby Protein Blot Stain. Directly after the transfer, the membrane was dried for a few minutes on a piece of filter paper, then wet in 95% ethanol until the membrane was no longer splotchy (about 10 seconds). The membrane was shaken face-down in a 50-mL solution of 7% acetic acid and 10% methanol in dH_2O, then shaken 4 times for 5 minutes in 100 mL of dH_2O. Next, the membrane was shaken face-up in a petri dish containing 15 mL of SYPRO® Ruby Protein Blot Stain. The excess stain was removed in 3 1-minute washes in 100 mL dH_2O. The membrane was dried again, then imaged using Bio-Rad Molecular Imager ChemiDoc XRS+ with Image Lab Software (Bio-Rad, Hercules, CA, USA) (all blot images were taken with this instrument).

2.6.6 Western blot

Immediately following the total protein stain, the membranes were blocked in 5% skim milk powder in Tris-buffered saline with Tween® 20 (TBST: 2.42 g Tris-HCl and 8.01 g NaCl in 800 mL of dH_2O, pH to 7.6, filled to 1 litre with more dH_2O, and 1 mL of Tween-20). The OxyBlot membranes were blocked (unshaken) overnight at 4 °C and the SOD-2 membranes were blocked and shaken for 1 hour at room temperature.

The primary antibody incubations also differed between the two blots; the OxyBlot membranes were incubated in 20 mL of 1:150 Rabbit Anti-(DNP) Antibody in TBST for 1 hour at room temperature, and the SOD-2 membranes were shaken on an MTS 4 shaker (IKA, Staufen, BW, Germany) in 5 mL of 1:500 Recombinant Anti-SOD2/MnSOD antibody

in TBST with 0.02% (w/v) NaN_3 overnight at 4 °C. Since the incubation volume was so low for the SOD-2 membranes' primary incubation, they were completed in small pouches made using Seal-A-Meal bags and a Plastic Film Sealer (PFS-200) (Shenlin, Shenzhen, GD, China).

The membranes were washed multiple times in 100 mL of TBST following the antibody incubations. The washing steps for the OxyBlot membranes were once for 15 minutes, then twice for 5 minutes; and the washing steps for the SOD-2 membranes were 4 times for 4 minutes. All the washing and subsequent steps were performed at room temperature.

For the secondary antibody incubations, the OxyBlot membranes were shaken for 1 hour in 20 mL of 1:300 Goat Anti-Rabbit IgG (HRP-conjugated) in TBST. The SOD-2 membranes were also shaken for 1 hour, but in 20 mL of 1:3000 Goat anti-rabbit IgG (H+L)-HRP Conjugate in TBST. The above wash steps were then repeated.

The chemiluminescence step was the same for both membranes. They were incubated in 10 mL of the substrate solution (1:1 Clarity™ Western enhanced chemiluminescence (ECL) Substrate Peroxide solution and Clarity™ Western ECL Substrate Luminol/enhancer solution) for 5 minutes. The still-wet blot was placed inside a sheet protector and imaged.

2.6.7 Stripping blots

When the chemiluminescence imaging did not turn out as planned, the blots were stripped following a mild stripping protocol. The membranes were left in TBST overnight at 4 °C, then washed 4 times for 5 minutes in 100 mL of TBST. They were blocked in 2%

skim milk powder in TBST for 30 minutes at room temperature. Finally, the above antibody incubation, washing, and imaging steps were repeated.

2.7 4-HNE assay

The 4-HNE ELISA was performed following protocol 2.5. The 4-HNE ELISA Kit (except for the Concentrated HRP Conjugate 100X) was warmed to room temperature for about 20 minutes prior to use. After warming up, the Concentrated Biotinylated Detection Antibody (100X) was spun down at 800 x g and 19 °C for 1 minute in the Centrifuge 5424 R, then diluted to 1X (4.5 µL of the antibody in 445.5 µL of the Biotinylated Detection Antibody Diluent was sufficient for 8 wells in the Micro ELISA Plate).

The protein-quantified worm samples (50 µL) (diluted as needed, but usually undiluted or diluted to 1 mg/mL of protein) and the kit's Reference Standards (20, 10, 5, 2.5, 1.25, 0.63, and 0 ng/mL 4-HNE) were added to the Micro ELISA Plate 15 minutes later. Fresh 1X diluted Biotinylated Detection Antibody solution (50 µL) was immediately added to each standard and sample well. The wells were sealed with tape and incubated at 37 °C for 45 minutes.

After a 10-minute pause, the Concentrated HRP Conjugate 100X was left to warm to room temperature over 20 minutes. It was then spun down at 800 x g and 19 °C in the Centrifuge 5424 R for 1 minute, then diluted to 1X (8.5 µL of the antibody in 841.5 µL of the HRP Conjugate Diluent was sufficient for 8 wells in the Micro ELISA Plate). In the meantime, 30 mL of the Concentrated Wash Buffer (25X) was diluted to 1X with 720 mL of dH_2O.

At the end of the Biotinylated Detection Antibody incubation, the solution was decanted from each well and the wells were washed 3 times for 1 minute with 350 µL of

the 1X wash buffer. Care was taken to remove residual bubbles and wash buffer from the wells, but also to avoid having the wells dry out between steps.

Fresh 1X diluted HRP Conjugate Diluent solution (100 µL) was then added to each standard and sample well. The wells were sealed with tape and incubated at 37 °C for 30 minutes, then washed 5 times following the above wash steps.

Next, Substrate Reagent (90 µL) was added to each of the wells. The wells were again covered with tape, and the plate was covered with tin foil to protect it from light. The plate was incubated at 37 °C for 15 minutes, then 50 µL of Stop Solution was added to each well in the same order that Substrate Reagent was added. The optical density of each well was immediately determined on a SpectraMax 340 Microplate Spectrophotometer set to 450 nm.

2.8 Live worm assays (survival, rescue, and fluorescence)

Figure 2.3 Age-synchronized L4 *C. elegans*, ready to be chunked for a survival test.

Tests requiring live nematodes were completed with about 20 nematodes per centrifuge tube containing 50 µL of increasing concentrations of paraquat. A range of paraquat concentrations were tested in the survival assays, then the lethal concentrations for 10, 50, and 90% of the population (LC10, LC50, and LC90) were calculated (30, 150, and 270 mM, respectively) and used in the rescue and fluorescence assays. In each test, at least 20 L4 worms were isolated by chunking them onto an unseeded, fresh plate. After ensuring there were no dead worms on the small chunk, 40-50 µL of test solution was pipetted on the top of the chunk, then deposited into 2 mL centrifuge tubes. Paraquat (0.5-2 M) was added to the tubes after the worms were washed in using the test solutions. The test solutions, paraquat concentrations, and exposure times varied by method. Each concentration of paraquat for each metd was performed in triplicate (except for the 500

mM paraquat survival assay test and the fluorescence assays, each of which were only completed once per worm strain).

2.8.1 Survival assay

The test solutions used in the survival assays were 0, 10, 25, 50, 100, 250, and 500 mM paraquat. Worms were initially taken off the chunk with M9 solution, then paraquat was added to the tubes containing worms to get them each to the proper concentration. The tubes were placed vertically on an MTS shaker and shaken for 2.5 hours at room temperature (each shaking step in the live worm assays were completed on this shaker). They were then dripped onto a clean agar plate and counted for survival under a Nikon Eclipse E200 Educational Microscope (Nikon, Konan, TYO, Japan). The worms were marked as alive if they were moving, or if they moved their head or tail when prodded with the worm picker.

2.8.2 Rescue assay

The test solutions used in the rescue assay were 10 mg/L antioxidant (either N-acetyl cysteine or Trolox, both in M9). Trolox is a carboxylic acid that only completely dissolves at a neutral pH, so 2 M NaOH was added to the Trolox solution until it dissolved at a pH of 7.2. The worms were shaken in the antioxidant solutions for 2 hours before the addition of paraquat, achieving final paraquat concentrations of 0, 30, 150, and 270 mM (negative control, LC10, LC50, and LC90, respectively). The worms were then checked for survival on the optical microscope.

2.8.3 Fluorescence assay

The test solutions used in the fluorescence assay were 0, 30, 150, and 270 mM. Paraquat (0.5-2 M) was added to each positive control tube at 30-minute intervals; for

example, paraquat was only added to the 150 mM worm sample 30 minutes after the addition of paraquat to the 30 mM sample. After each tube was exposed to paraquat for 2.5 hours, 1 µL of 2.5 mM H_2-DCFDA in DMSO (stored in the dark at -20 °C) was added to each sample, resulting in a final concentration of 50 µM H_2-DCFDA. *C. elegans* can tolerate DMSO concentrations of up to 2% [81]. The worms were incubated for an additional 3.5 hours in the stain, then were anaesthetized (again at 30-minute intervals) with 5 µL of 10 mM levamisole hydrochloride in water (stable for 90 days at 4 °C), obtaining a final concentration of about 1 mM levamisole (a suitable concentration for stress experiments) [82]. The worms were imaged immediately using the 10X magnification of an EVOS FL Imaging System (AMF4300) (Thermo Scientific, Rockford, IL, USA). The images were obtained using light transmission (at 14% transmitted light) or fluorescence (using the GFP setting, with 470 nm excitation and 525 nm emission; and the exposure settings at 60% light intensity and 80 ms exposure time).

2.9 Oxylipin assay

Deionized water (diH_2O) was prepared using a PURELAB® Flex 2 (Elga, High Wycombe, Bucks, England) and added to the methanol-samples from protocol 2.4 until the diH_2O:methanol ratio in the samples was 80:20. For example, 2 mL of water was added to 500 µL methanol-based samples.

2.9.1 Oxylipin extraction

Oasis HLB 3 cc (60 mg) Extraction Cartridges (Waters, Milford, MA, USA) were added to a solid phase extraction (SPE) vacuum manifold with a slight vacuum pressure, and cleaned with 1 column volume of HPLC-grade methanol, then 2 column volumes of

HPLC-grade ethyl acetate. The cartridge was then conditioned with 2 column volumes of 80:20 diH_2O:methanol, ensuring the solid phase (the frit) never went dry.

The 80:20 diH_2O:methanol nematode samples were then added to the cartridge. Two more column volumes of 80:20 diH_2O:methanol were added to the cartridge, each just before the top of the liquid arrived at the frit. After the second solvent addition, the frit was dried for 10 minutes at a vacuum pressure of 10 inHg.

Meanwhile, 6 µL of trapping solution (30% glycerol in LC-MS-grade methanol) was added to 2 mL centrifuge tubes. These centrifuge tubes were placed underneath the dried cartridges, then 0.5 mL HPLC-grade methanol was passed through the cartridges to begin eluting the oxylipins. HPLC-grade ethyl acetate (1.5 mL) was added just before the methanol layer reached the top of the frit. A slight vacuum pressure was applied to collect the eluate, then the collected samples were dried down on a Vacufuge™ Concentrator (Eppendorf, Hamburg, HH, Germany) at 30 °C (about 45 minutes). The samples were reconstituted with 60 µL of LC-MS-grade methanol and stored at -20 °C.

2.9.2 UPLC-MS/MS Analysis

The samples from protocol 2.9.1 were further purified by their transfer to Ultrafree-MC Centrifugal Filter tubes (with Durapore® PVDF 0.1 µm, from Merck Millipore, Tullagreen Carrigtwohill, IE-M, Ireland) and a 10-minute spin on the Centrifuge 5424 R at 13200 x g and 4 °C. Chromatographic separation was performed using an Acquity UPLC BEH C18 column (50 × 2.1 mm; 1.7 µm) (Waters, Milford, MA, USA). The analysis was carried out using a Waters Acquity UPLC I-Class System coupled to a Waters Xevo TQS-micro Triple Quadrupole Mass Spectrometer operating in negative electrospray ionization mode. Samples were injected (5 µL) and separated using a gradient method over 19 min

at 0.3 mL/min using acetonitrile and H_2O:acetonitrile (95:5) mobile phases, each containing 0.1% formic acid (all solvents were LC-MS-grade). Quantification of oxylipins was calculated from constructed calibrations curves for each analyte, and normalized to the response of the respective deuterated internal standard.

3.0 Results and discussion

Both styrene and paraquat were used to induce oxidative stress in *C. elegans*, though worms exposed to styrene did not consistently show changes between the negative and positive controls. After styrene-exposed worms were tested in a few different assays (SOD-2 expression, protein carbonylation, and 4-HNE production), the toxicant was switched to paraquat, which induced deaths and oxidative stress in worms.

3.1 Styrene

Styrene was initially used as the main pro-oxidant in the *C. elegans* assays. Since it is activated by CYP2E1, the oxidative stress observed between the three worm strains was expected to increase in mtCYP2E1 worms (due to bioactivation in the mitochondria, leading to mitochondrial dysfunction), be slightly less in erCYP2E1 worms (due to bioactivation in the cytosol, with less mitochondrial dysfunction); and be the least in N2 worms (which lack CYP2E1, so styrene is less likely to be bioactivated). In each of the three oxidative stress testing methods (protein carbonylation, SOD-2 expression, and 4-HNE production), there was never a significant difference between the negative (solvent) control and the styrene-treated worms.

3.1.1 Protein carbonylation

After multiple trials testing the protein carbonylation in *C. elegans* samples (the last of which are shown in Figure 3.1), it was clear that there are already many carbonyl groups on proteins that have not undergone oxidative distress. The many carbonyl groups observed in negative control samples resulted in significant background protein oxidation observed in protein carbonylation tests. Sample preparation is a major contributor of artifacts of oxidative stress; proteins are quickly oxidized after cellular lysis. Different methods were used to minimize oxidation during sample preparation to reduce background protein oxidation, including adding a reducing agent (either 50 mM DTT or 1-2% 2-mercaptoethanol) to the lysis buffer, adding a reducing agent to the OxyBlot samples immediately after DNP-derivatization, and changing lysis methods from boiling to beat beating. These methods are discussed below.

The first of these adjustments—adding a reducing agent during lysis—made the samples incompatible with the BCA assay (which only tolerates up to 0.01% 2-mercaptoethanol), so the samples' protein concentration could not be quantified. Without quantification, the protein mass loaded onto the gel for SDS-PAGE may not be consistent between samples. However, the Bradford assay is more compatible with reducing agents, so it was explored as an alternative to the BCA assay [83]. Ultimately, because the BCA assay was already producing consistent results, it remained the chosen method for protein concentration. In the following experiments, no reducing agent was added during sample lysis.

Following the OxyBlot manufacturers' recommendations, 2-mercaptoethanol was added later in sample preparation, instead [84]. After derivatization with DNP, protein

samples were reduced with 5.5% 2-mercaptoethanol. While adding a reducing agent after derivatization did not have any detrimental effects on blot resolution, there was still significant background in negative control samples.

Another contributor to the protein oxidation observed in the solvent control samples may have been the lysis method; worms were boiled for 10 minutes to break down their thick cuticle and release proteins. Since heat effects generate ROS, the extended boiling likely increased the oxidative stress and protein carbonylation in the samples [85]. After observing these heat effects, *C. elegans* were homogenized using a bead beater, keeping each step as cold as possible.

Figure 3.1—which shows the protein carbonylation in mtCYP2E1 worms exposed to M9 (blank control) or styrene in M9 (at 500 μM)—is the result of months of OxyBlot optimization. The same worm samples (N=4 technical replicates, where 4 lanes were loaded per sample) were run one week (W1) and again the next (W2). Separating the results by week was intentional; it shows how OxyBlot tests produced inconsistent results, even within a single sample in a one-week period. In the first set of results, there was a significant ($p<0.05$) decrease in protein oxidation in the styrene-exposed samples, implying that styrene has a protective effect on oxidative stress. However, these results were shifted the following week, which did not show a significant difference between the controls.

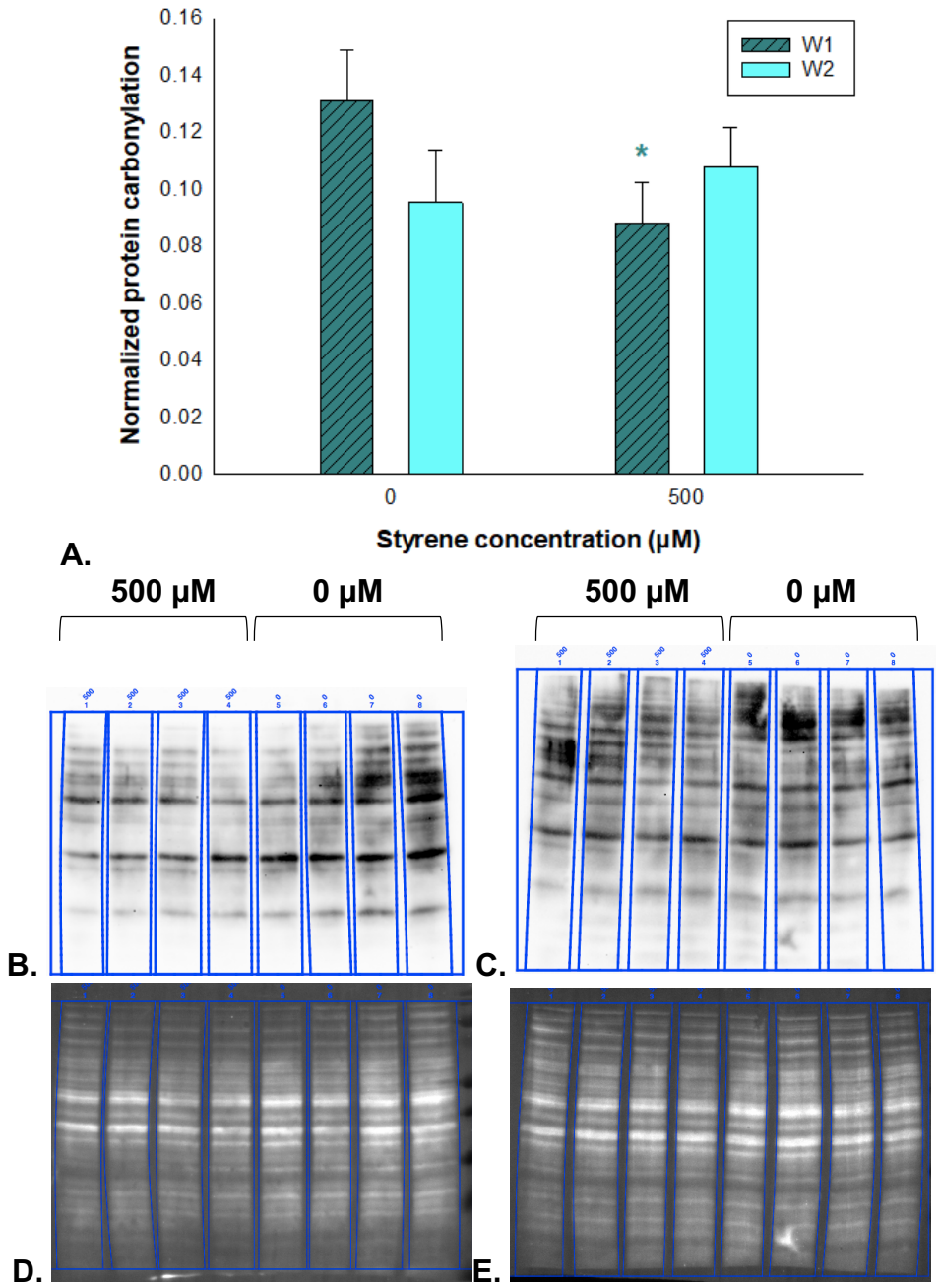

Figure 3.1 (A) Protein carbonylation observed in mtCYP2E1 worms exposed to M9 and 500 µM styrene in M9 (N=4 technical replicates). The same worm sample was run one week (W1) and again the next (W2). The worms were lysed using glass beads in a bead-beater. In the first week, there was a significant ($p<0.05$) reduction in protein carbonylation in worms exposed to styrene (relative to the solvent control), though this result was not repeated the following week. (B) and (C) show the chemiluminescence of W1 and W2 proteins, respectively, where the worms were incubated in 500 (lanes 1-4) and 0 (lanes 5-8) µM styrene in M9. (D) and (E) show their respective corresponding total protein stains.

The high background produced in OxyBlots has been discussed in literature. Protein carbonylation can also be artificially increased by nucleic acid contamination—something that is likely to occur during cell lysis [40]. The reformulation of OxyBlot kits has also resulted in decreased sensitivity and a lack of reproducibility, relative to previous versions of the kit [41]. For these reasons, further OxyBlot tests were paused and the project focus was shifted toward another oxidative stress biomarker: antioxidant gene expression.

3.1.2 SOD-2 expression

Since SOD-2 converts $O_2^{\bullet-}$ (a radical ROS) to the less-reactive H_2O_2, it has a role in the oxidative stress response and may be upregulated to reduce ROS during increased oxidative stress. Its expression was measured by western blot, meaning that an antibody targeting *C. elegans*' SOD-2 was needed. However, antibodies are typically grown in mammals, meaning that any antibodies that are purchased for *C. elegans* may only result in non-specific binding. Luckily, one primary antibody (ab68155) showed high specificity with *C. elegans* SOD-2, resulting in clean bands at the correct molecular weight (22 kDa). There was a slight increase in SOD-2 expression in styrene-exposed erCYP2E1 worms, though it was not significant, while styrene-exposed mtCYP2E1 worms showed a very significant ($p<0.001$) decrease in SOD-2 expression (Figure 3.2). This change was the opposite of what was expected to happen; since styrene metabolism produces ROS that are detoxified by SOD-2, SOD-2 expression was expected to increase to balance the added oxidative stress.

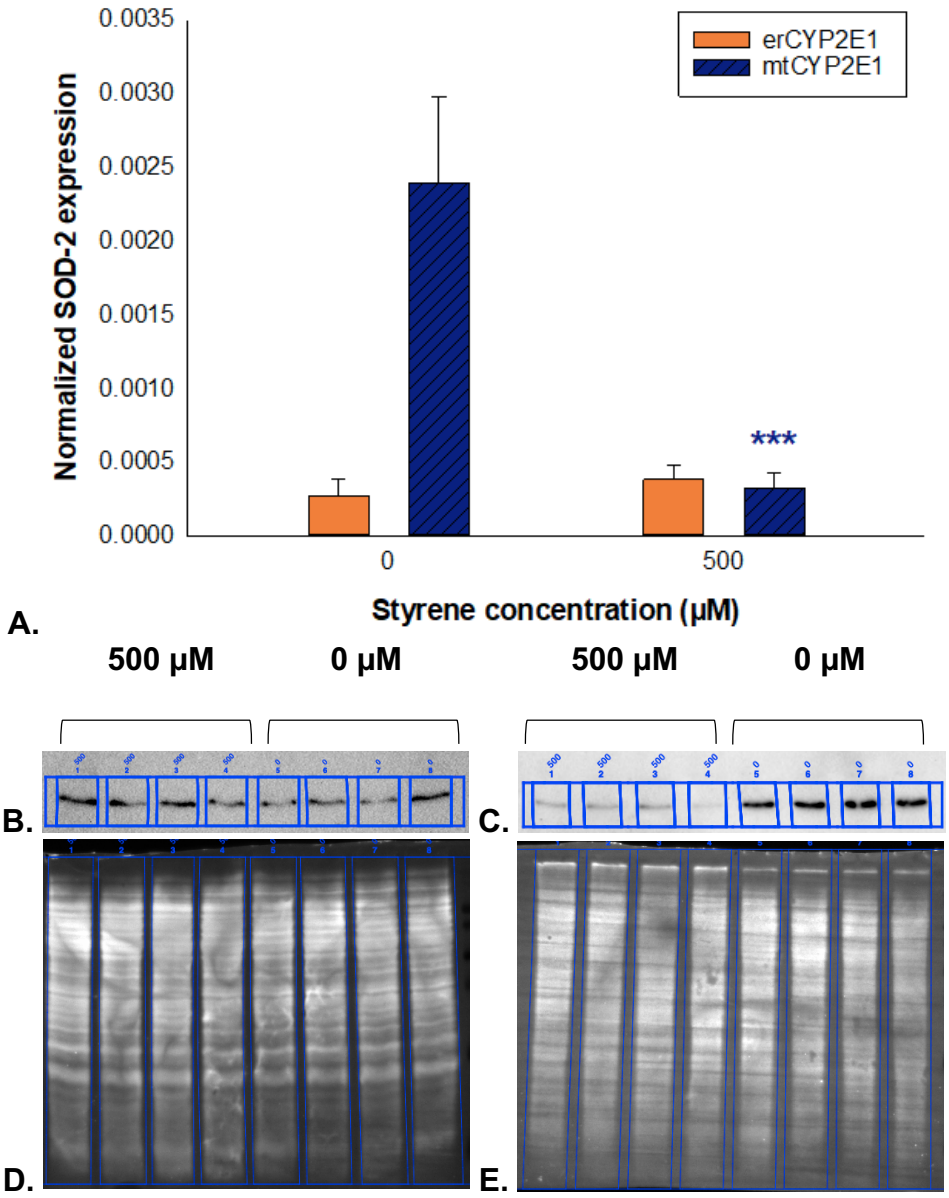

Figure 3.2 (A) SOD-2 expression was measured by chemiluminescence in erCYP2E1 and mtCYP2E1 worms exposed to 0 and 500 μM styrene in M9 buffer (N=4 technical replicates). The worms were lysed using glass beads in a bead beater. There was a very significant ($p<0.001$) reduction in SOD-2 expression in mtCYP2E1 worms exposed to styrene (relative to the solvent control) while there was no change in SOD-2 expression in erCYP2E1 worms. (B) and (C) show the chemiluminescence of SOD-2 bands (incubated in 500 (lanes 1-4) and 0 (lanes 5-8) μM styrene in M9) in erCYP2E1 and mtCYP2E1 worms, respectively, while (D) and (E) show their respective total protein stains. The full images of the chemiluminescence blots are shown in Figures S.1 and S.2.

There are a few reasons why SOD-2 expression could have remained unchanged. First, SOD-2 is constitutively expressed, so any induction of the protein's expression needs to be enough to differentiate it from its expression in negative control samples [86]. There is also evidence that alternate detoxifying mechanisms are used when SOD-2 is inhibited. While SOD-2 RNA interference (RNAi) made some *C. elegans* mutants more vulnerable to paraquat toxicity, it increased the longevity of a mitochondrial mutant [87]. It is possible that *C. elegans* SOD-2 expression decreases or does not change upon exposure to styrene; however, the lysis method was upgraded once again to ensure these results were accurate.

Instead of homogenizing with glass beads, subsequent *C. elegans* lysates were prepared using ceramic beads. Though they are more expensive, ceramic beads are better-suited for homogenizing plant and animal materials than glass beads, which are suitable for lysing microorganisms [88]. SOD-2 expression was quantified in mtCYP2E1 worms lysed by one of two ceramic bead kits: mixed (M) beads, which contained both 1.4 and 2.8 mm diameter beads; and uniform (U) beads, which contained only 2.8 mm diameter beads (Figure 3.3). The styrene-treated samples were also exposed to a 10X-increased concentration of styrene, at 5000 μM. A reduction in SOD-2 expression was observed again but only in the worms lysed with uniformly-sized beads and not in those lysed with mixed-size beads. The two lysis methods are similar; the only difference is the mixed-bead kit contained 1.4 mm diameter beads, which are better able to grind up soft tissue (whereas 2.8 mm beads are better able to homogenize hard tissue, such as cartilage) [88].

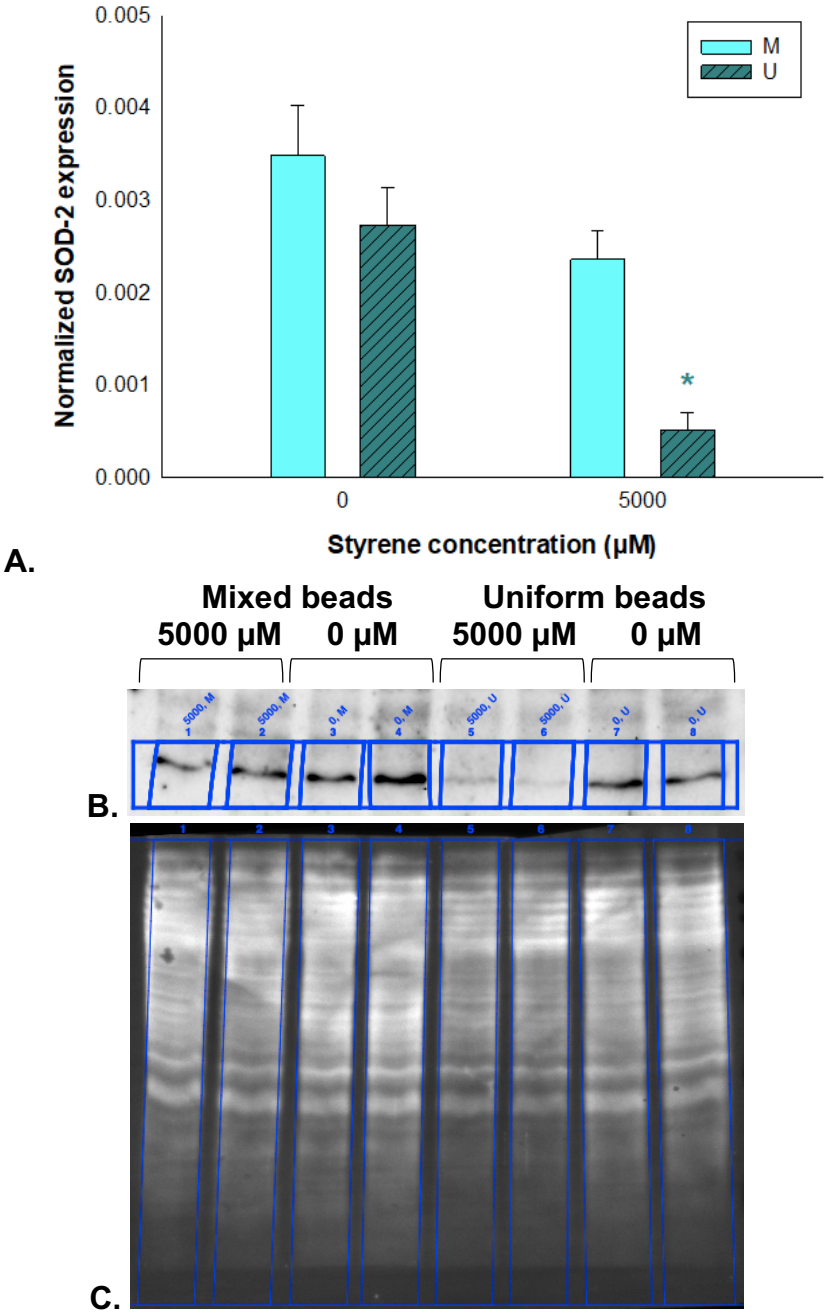

Figure 3.3 (A) SOD-2 expression in styrene-exposed mtCYP2E1 worms lysed using two ceramic bead kits; mixed-size beads (M, at 1.4 and 2.8 mm) and uniformly-sized beads (U, at 2.8 mm) (N=2 technical replicates). There was a significant ($p<0.05$) reduction in SOD-2 expression in worms exposed to 5000 μM styrene; however, this effect was only observed in the U sample. (B) The chemiluminescence of SOD-2 and (C) corresponding total protein stain of worms incubated in 5000 (lanes 1-2, 5-6) and 0 (lanes 3-4, 7-8) μM styrene in M9, then lysed by either mixed- (M) (lanes 1-4) or uniformly- (U) (lanes 5-8) sized ceramic beads. The full image of the blot is shown in Figure S.3.

The different SOD-2 expressions observed in Figure 3.3 could be explained by slight differences in the proteins released from the soft and hard tissue, though the negative solvent control of both lysis methods started out with similar levels of SOD-2 expression. Instead, the continued inconsistencies in SOD-2 expression could be that the styrene exposure method was not causing sufficient oxidative stress to induce or inhibit SOD-2 expression.

The exposure method used for styrene may not have been sufficient to induce an oxidative stress response in the worms. They remained on sealed agar plates, where they were dosed with styrene every 12 hours for 48 hours. Despite being sealed with Parafilm, the plates may have released enough styrene over 12 hours that the worms were not in stress conditions.

Alternatively, the liquid styrene could have diffused into the agar plate rather than remain on top, where the worms were. The sinking effect would have occurred more readily on older, dry plates, so the plates used in these tests were always around the same age. Agar plates used in *C. elegans* toxicity tests can be impregnated with toxicants to counteract this sinking effect, but if the toxicant is a volatile compound like styrene, the impregnation would have to be done after the media is sterilized. When this was attempted with styrene, it made the plates more susceptible to bacterial and fungal contamination, something that was already a problem during the long styrene exposure tests (where about 2 mL of liquid would sit on the worm plate over 48 hours). Given the volatility of styrene and the difficulty in controlling the concentration of volatile toxicants on agar plates, the toxicant and exposure method were switched.

3.1.3 4-HNE production

Each time 4-HNE production was tested by a competitive ELISA, the sample signals were below the detection range of the assay (0.63-40 ng/mL). Despite an improved lysis method (ceramic beads rather than glass beads), increased toxicant concentration (by 10X), different toxicants (paraquat and styrene), and improved exposure method (immersion in the toxicant rather than exposure on agar plates), there were never 4-HNE signals in either the negative or positive control that were high enough to compare to one another (a representative example is shown in Figure S.4).

The aldehyde products of lipid peroxidation readily conjugate to biomolecules, so the concentration of free 4-HNE *in vivo* is likely to be low [44]. The antibodies in the 4-HNE ELISA kit from Elabscience detect free 4-HNE rather than 4-HNE conjugated to proteins, so it's possible that much of the 4-HNE produced in *C. elegans* was missed. There are a couple other studies that also reported low 4-HNE concentrations after using a 4-HNE ELISA kit by the same manufacturer (0.00132 and 0.58148 ng/mL in serum [89], and 2 ng/mL in epithelial cells [90]), though it is unclear whether the kits contained the same antibodies. Alternatively, there may not have been enough biomass used in the *C. elegans* assays, though each sample had at least 3 mg/ml protein. If further testing with this ELISA is done, it should be completed with a higher concentration of worms that have been grown in liquid culture.

3.2 Paraquat

As mentioned above, paraquat is a well-known pro-oxidant that is commonly used to induce oxidative stress in models. When neither styrene nor ethanol affected oxidative stress biomarkers (protein carbonylation, antioxidant gene expression, and lipid

peroxidation), the toxicant was switched to paraquat. Although paraquat is not metabolized or activated by CYP2E1 and is unlikely to affect the worm strains differently, it was chosen as a “proof-of-concept” control (given its high toxicity and use as a pro-oxidant) to develop these oxidative stress assays in *C. elegans*.

3.2.1 Survival assay

Survival dose-response assays were run on each *C. elegans* strain, where they were incubated in test solutions for 2.5 hours (Figure 3.4). Each dose for each strain was repeated 3 times using at least 20 worms per replicate. As expected (since paraquat is not activated by CYP2E1), there were few differences in the survival rates between worm strains (see table S.2). While mtCYP2E1 survival in 50 mM paraquat decreased significantly ($p<0.05$) relative to the N2 worms, mtCYP2E1 experienced greater survival than N2 at higher doses. The survival rates were fitted using non-linear regression, which were sigmoidal dose-response curves. Paraquat exposure caused a significant ($p<0.001$) drop in average survival rates at the two highest doses (250 and 500 mM), and the survival rates at lower doses were comparable to those seen in other *C. elegans* paraquat survival assays [38, 91].

Since paraquat was shown to cause deaths in *C. elegans*, additional assays that provide information on the toxic mechanism can be performed at appropriate doses. The linear portion of this dose-response curve (with the averaged survival rates of each strain) was used to calculate the LC10, LC50, and LC90 that could be used in subsequent experiments. When most of the survival assays were completed, the LC10, LC50, and LC90 values were approximately 30, 150, and 270 mM. These values are only approximate because there was some (insignificant) variation in survival rates between

strains at the 250 mM dose, and some of the replicates used to calculate the doses did not include at least 20 worms.

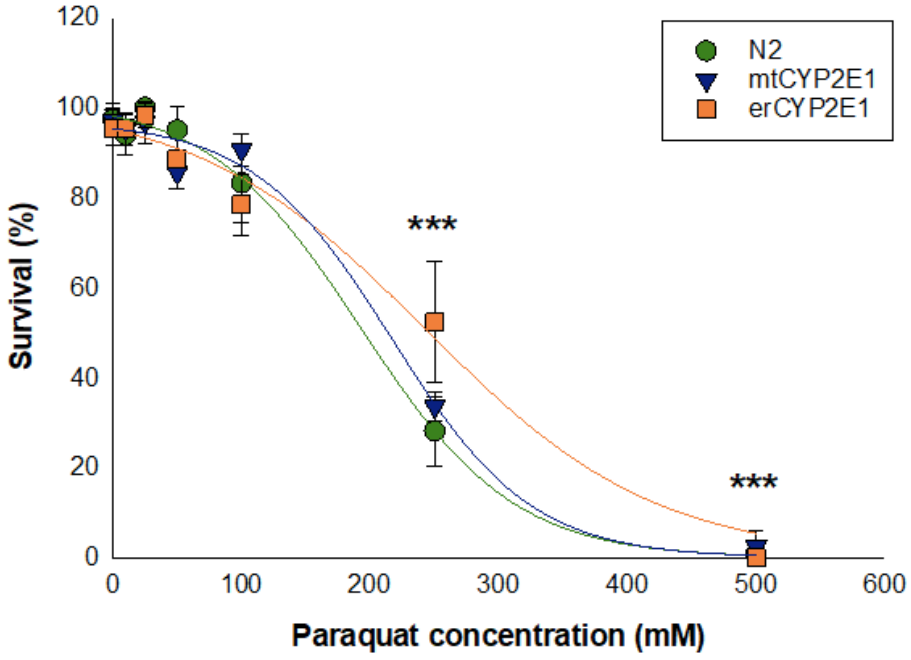

Figure 3.4 Wild-type (N2), erCYP2E1, and mtCYP2E1 worm survival was measured after 2.5 hours after swimming in increasing paraquat concentrations (N=3). There was no significant difference in survival between the strains, at any doses. 250 and 500 mM paraquat exposure caused significant ($p<0.001$) drops in the average survival rate.

Since then, additional replicates have been performed to replace the trials that did not use enough worms, and those replicates have influenced the LC values slightly (to 45, 200, and 350 mM, respectively). However, the initially-calculated paraquat LC values were used in the next set of experiments.

3.2.2 Rescue assay

The first of these experiments was a rescue assay, where each *C. elegans* strain was incubated with ROS scavengers such as Trolox (TA) or N-acetyl cysteine (NAC) for 2 hours prior to the addition of either 0, 30, 150, 270, or 500 mM paraquat (Figure 3.5). Each test was run in triplicate for each strain, then averaged.

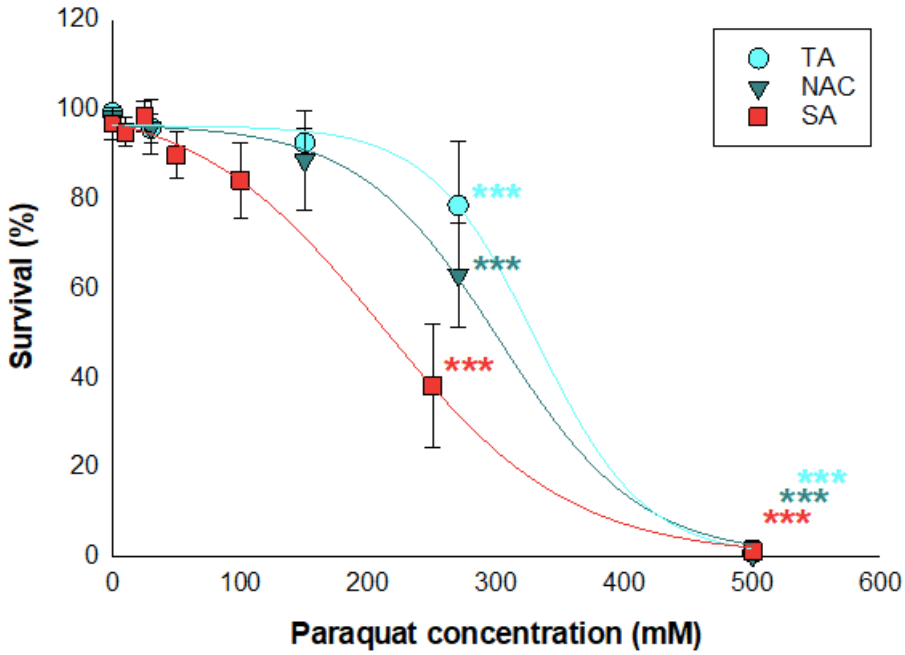

Figure 3.5 The average survival rate of *C. elegans* strains incubated in either Trolox (TA) or N-acetyl cysteine (NAC) prior to the addition of paraquat (N=3 individual experiments, with at least 20 worms per experiment). The average survival rates of worms without prior antioxidant exposure are also displayed (SA). Like in the survival assays, there was significantly ($p<0.001$) reduced survival in the rescue assays at both 270 mM and 500 mM paraquat. However, the median lethal paraquat doses increase when worms are first incubated in either antioxidant.

Like in the survival assay, worms incubated in either antioxidant experienced significantly reduced survival at both 270 and 500 mM paraquat. The LC values of the worms incubated in Trolox and N-acetyl cysteine increased by 326% and 109%, respectively (to an LC10, LC50, and LC90 of about 160, 890, and 1620 mM paraquat for Trolox worms; and 90, 420, and 750 mM for N-acetyl cysteine worms, compared to 45, 200, and 350 mM calculated in the survival assays). However, the near total worm death at the high dose (500 mM paraquat) confirms that the higher LC values calculated using only the linear portion of the dose-response curve are unrealistic. Though antioxidant incubation cannot perpetually avoid deaths caused by paraquat, it can delay the deaths. Since antioxidant incubation increased survival rates in worms exposed to paraquat, it is likely

that paraquat induced death by increasing oxidative stress. Therefore, this rescue assay shows that subsequent *C. elegans* tests using these paraquat concentrations experience increased oxidative stress.

3.2.3 Fluorescence assay

Now that there is evidence showing paraquat causes deaths in *C. elegans*, and those deaths are rescued by antioxidant incubation, the next step was to examine what was happening inside the worm by quantifying ROS. ROS were measured by fluorescence in each worm strain following exposure to 0, 30, 150, and 270 mM paraquat (Figures 3.6 and 3.7). Each concentration used at least 6 worms, except for erCYP2E1 worms exposed to 30 mM paraquat, which only had 3 worms tested. There was a median of 9, 20, and 12 worms tested for the mtCYP2E1, N2, and erCYP2E1 strains, respectively.

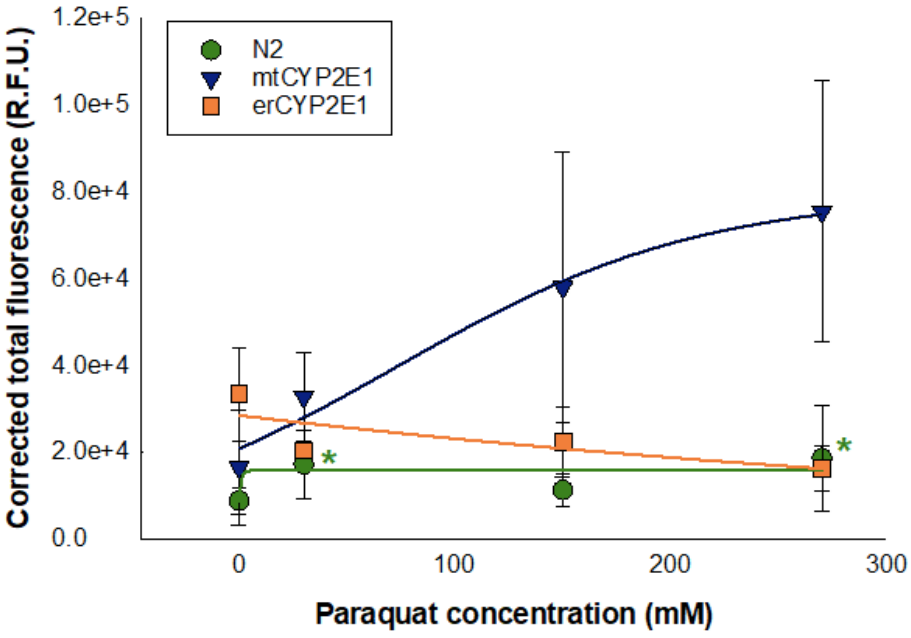

Figure 3.6 Corrected total fluorescence (in relative fluorescence units, or R.F.U.) of 2',7'-dichlorofluorescein measured in N2, erCYP2E1, and mtCYP2E1 worms exposed to 0, 30, 150, and 270 mM paraquat (N=1 test, with ≥ 3 worms per test).

There is variation in the number of worms observed because worms that were clumped with other worms or next to bright artifacts (typically gel fragments) in the agar plate were not counted, since those effects can alter the fluorescence observed in individual worms. Outliers were also removed from each dataset. There was a very significant increase in ROS production in LC90 N2 worms relative to the negative control worms ($p<0.001$). There were also significant ($p<0.05$) increases in ROS production between individual doses (negative control and LC10, and LC90 and LC50). There was also an overall upward trend in ROS production in mtCYPE1 worms (relative to the negative control worms, the LC50 and LC90 worms had a very significant ($p<0.001$) increase in ROS production). The fluorescence observed in erCYP2E1 worms was the opposite, where LC50 and LC90 worms experienced a significant ($p<0.05$ and $p<0.001$, respectively) reduction in ROS production. The trends observed across the strains were different even though paraquat is not metabolized by CYP2E1.

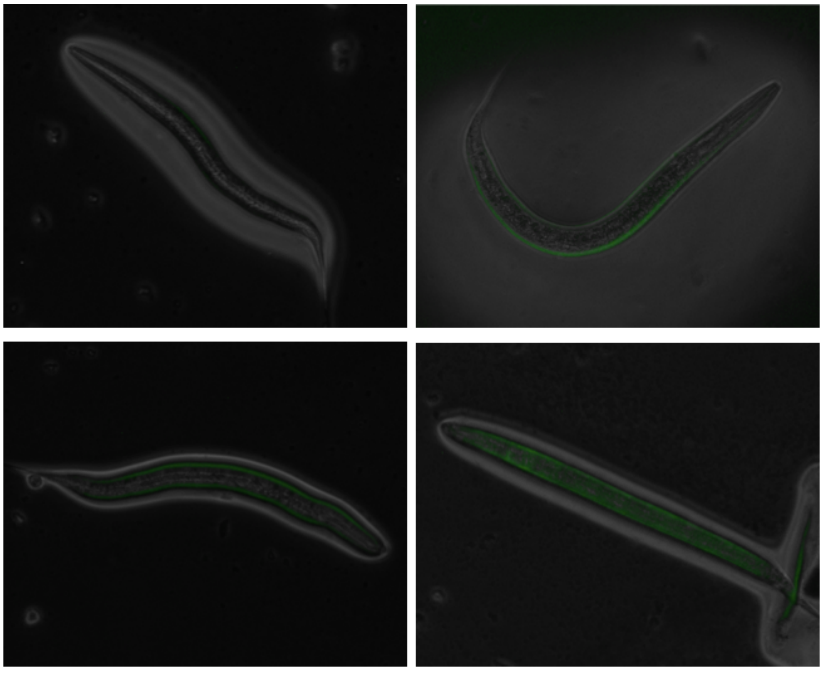

A. mtCYP2E1

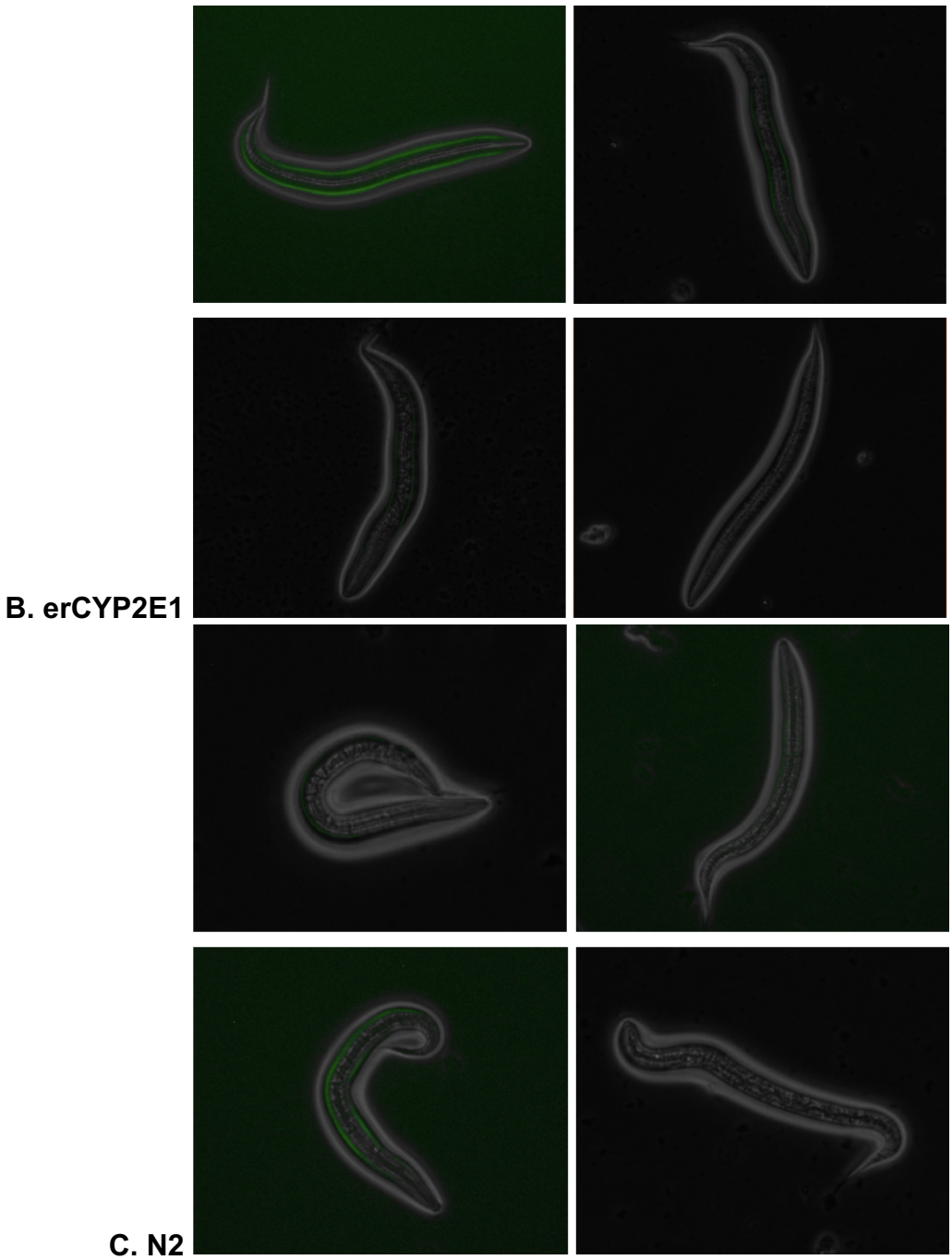

Figure 3.7 Representative overlay (fluorescent over visual light) images of mtCYP2E1 (A), erCYP2E1 (B), and N2 (C) worms exposed to 0, 30, 150, and 270 mM (from left to right) paraquat. Most of the fluorescence appears to be in the worms' body wall muscles.

These differences could be explained by the large standard deviation observed at each dose resulting from the low number of worms tested and interassay differences in procedure. Once additional replicates of each experiment are performed, there may be

more consistency in the different worms strains' response to paraquat. Alternatively, the differences may also be caused by uncoupling of CYP2E1 and the resulting mitochondrial dysfunction, although this warrants future exploration and increased biological replicates before further discussion can take place.

3.2.4 SOD-2 expression

Since the survival and rescue assays showed paraquat had clearly induced death and possibly oxidative stress, mtCYP2E1 worms exposed to the LC0, LC10, and LC50 (0, 30, and 150 mM, respectively) of paraquat were tested once again for SOD-2 expression (Figure 3.8). Like mtCYP2E1 worm incubations with styrene, there was a very significant ($p<0.001$) overall decrease in SOD-2 expression upon exposure to a pro-oxidant. Relative to the negative control, there was a very significant ($p<0.001$) decrease in SOD-2 expression in worms incubated in 30 mM paraquat; however, relative to those LC10 worms, there was a slight increase ($p<0.05$) in SOD-2 expression in worms incubated in 150 mM paraquat. A qPCR test using paraquat as a pro-oxidant showed no change in SOD-2 expression in mouse keratinocytes, so it is possible that SOD-2 expression is not significantly affected by paraquat [12]. Therefore, additional biological replicates are required to confirm that paraquat incubation induces a dose-dependent decrease in SOD-2 expression. Future testing could also include other antioxidant proteins like catalase, since its expression was significantly increased in the same test using mouse keratinocytes exposed to paraquat [12]. However, cells do not contain the same enzymes or toxicokinetics as whole organisms, so antioxidant protein expression in cells may be different than what is observed in *C. elegans*. Additionally, while western

blot shows the expression of antioxidant genes, it does not show how active the proteins are.

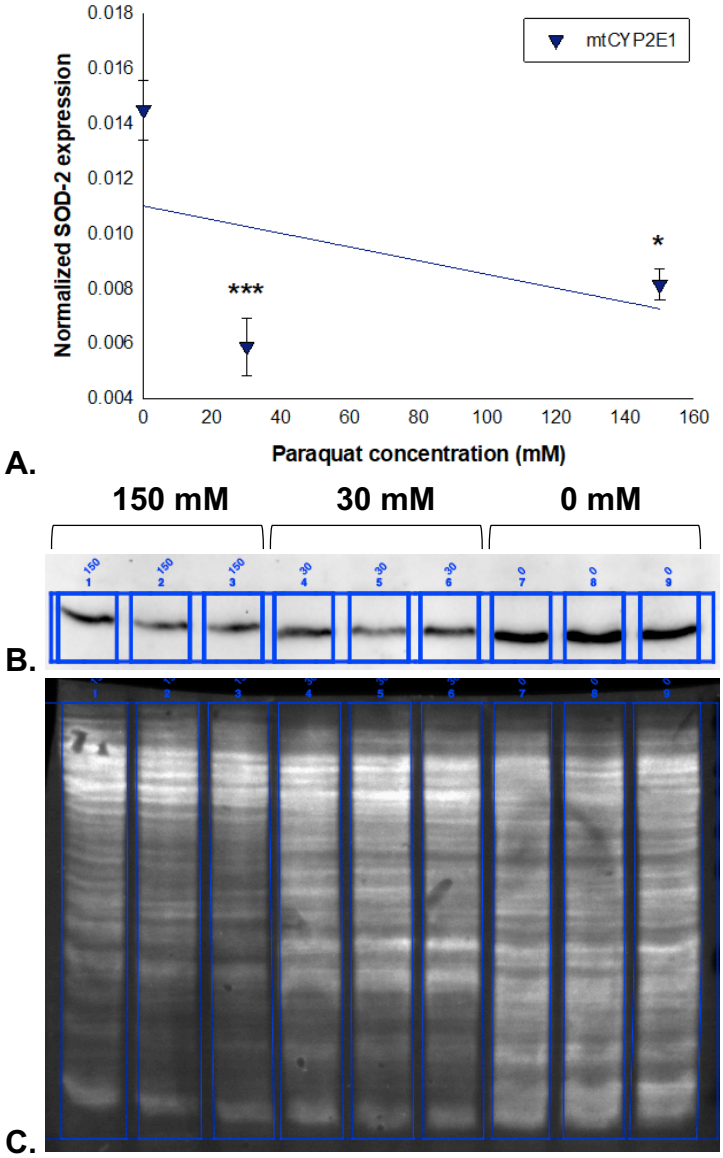

Figure 3.8 (A) SOD-2 expression in mtCYP2E1 worms exposed to 0, 30, and 150 mM paraquat in M9 (N=3 technical replicates). The worms were lysed using mixed-size ceramic beads in a bead beater. (B) The chemiluminescence of SOD-2 and (C) corresponding total protein stain of worms incubated in 150 (lanes 1-3), 30 (lanes 4-6), and 0 (lanes 7-9) mM paraquat in M9. The full image of the chemiluminescence blot is shown in Figure S.5.

In oxidative stress conditions, antioxidant proteins may be expressed but become inactive, so only measuring gene expression may not provide accurate information on the

state of oxidative stress in the organism [92]. A better way of monitoring oxidative stress is to monitor multiple biomarkers that are independent of protein expression, like the production of dozens of oxylipins.

3.2.5 Oxylipin assay

Until the oxylipin assays, all worms used for tests requiring homogenization (such as western blots and ELISAs) were grown on multiple agar plates (32 plates per dose). Worms were grown the same way for a preliminary UPLC-MS/MS run testing the oxylipin content of *C. elegans* exposed to 0, 30, and 150 mM paraquat (N=1). Most oxylipin signals were below the instrument's limit of detection (LODs for oxylipins ranged from approximately 0.06-3 ng/mL), so the samples could not be quantified. To test how close the samples were to the LOD, the samples were combined and concentrated 12X (table 3.1).

Table 3.1 Improved oxylipin detection in concentrated *C. elegans* samples by UPLC-MS/MS. The blue highlight indicates the oxylipins that were detected in both the initial control sample and the concentrated control sample.

Oxylipin class	Oxylipin	Control		12X concentrated control	
		Detected	Signal:Noise	Detected	Signal:Noise
EET	11-EET				38
	11-EpETE				11
	12-EpOME		51		194
	14-EET				
	14-EpETE				
	16-DPE				222
	19-DPE				
	7-DPE		7		27
	8-EET				29
	8-EpETE				
	9-EpOME		508		338
DHET	11-DHET				315
	11-DiHETE				14
	12-DiHOME				457
	14-DHET				185
	14-DiHETE				65
	16-DiHDPA				
	19-DiHDPA				30
	7-DiHDPA				
	8-DHET				146

	8-DiHETE		23
	9-DiHOME		308
	11-DHET		315
HETE	11-HETE		83
	12-HEPE		130
	12-HETE		90
	13-HODE	35	225
	14-HDHA		17
	15-HEPE		114
	15-HETE		357
	16-HDHA		93
	17-HDHA		15
	18-HEPE		152
	20-HDHA		1107
	20-HETE		
	4-HDHA		
	5-HEPE		14
	5-HETE		7
	8-HEPE		867
	8-HETE		3402
	9-HETE		37
	9-HODE	55	380
Leukotriene	LKB_4		
	LKD_4		
Lipoxin	Lipoxin A_4		22
oxoETE	9-oxoODE		466
	15-oxoETE		7
	5-oxoETE		89
Resolvin	Resolvin D_1		
PG	6-keto-$PGF_{1\alpha}$		
	PGD_2		3
	PGE_2		4
	PGE_3		
	$PGF_{2\alpha}$		5
Thromboxane	T_XB_2		6
Iso-P	5-$IPF_{2\alpha}$ -VI		754

Concentrating the samples 12X improved overall oxylipin detection by 66%. Even with the more concentrated samples, though, some oxylipin classes (including the EETs, leukotrienes, and PGs) were not detected. Knowing that samples need to be at least 12X will inform how many extra worms to grow for future runs, using liquid culture to propagate more worms to attain a biomass that is necessary to detect all oxylipin classes.

Once liquid culturing is optimized to produce signals that are above the LOD in each sample, oxylipin concentrations will be compared between each sample to see which oxylipins are most affected by increased oxidative stress. The most important

oxylipins to optimize are those that are already considered the gold standard for biomarkers of oxidative stress: the iso-Ps. Taking it a step further, the ratios of product oxylipins to their precursors (for example, 20-HETE to ARA, or 5-oxoETE to 5-HETE) will be calculated, which will allow for a more accurate comparison between worm samples and show how certain pathways are induced under oxidative stress conditions.

4.0 Conclusion and implications

Survival and rescue assays successfully demonstrated that the pro-oxidant paraquat caused death and oxidative stress, respectively, in *C. elegans*. The expression of SOD-2 (an antioxidant gene) was measured by western blot, and decreased significantly in worms incubated in paraquat. However, there were only three technical replicates so more testing needs to be completed to confirm the reduction in SOD-2 expression. Fluorescence assays showed increased ROS generation in mtCYP2E1 and N2 worms exposed to paraquat, but not in erCYP2E1 worms. These data suggest a link between the localization of CYP2E1 to the mitochondria and increased oxidative stress, but more biological replicates need to be completed across the 3 worm strains for this to warrant further discussion.

Styrene, which is metabolized by CYP2E1 to produce a more bioactive pro-oxidant, was used to assess further differences in ER- and mitochondrial-localized oxidative stress. However, the tests measuring the effects of styrene on oxidative stress biomarkers (protein carbonylation, SOD-2 expression, and lipid peroxidation) were inconclusive. While there were problems in optimizing each of these assays, it is likely that the styrene exposure method was the main reason for the lack of oxidative stress observed in styrene-exposed worms. To ensure worms are exposed to sufficient

concentrations of styrene, future tests should immerse worms in styrene rather than applying styrene to NGM plates containing worms. They should also begin with survival and rescue assays as those have already been validated using paraquat.

Using styrene to differentiate between the oxidative stress caused by mtCYP2E1 versus erCYP2E1 could allow for advances in drug development and toxicity testing. It is currently unknown which which of these isozymes drives oxidative stress and toxicity, what the role of CYP2E1 isozymes is in multiple pathologies (such as liver disease, heart disease, cisplatin-induced nephrotoxicity, and neurotoxicity), and what the relative expression of both CYP2E1 isozymes is in human tissues [29]. Clarifying these three data gaps would help in the development of pharmaceuticals that alleviate these diseases.

Additionally, the potential for mtCYP2E1 to play a key role in oxidative stress and disease progression makes it an important enzyme to monitor in toxicity testing. While *C. elegans* applications are being considered among new approach methodologies to animal testing, *C. elegans* and humans have different toxicokinetic pathways causing them to metabolize xenobiotics differently. To better predict the adverse effects of xenobiotics, test organisms must share as much in common with humans as possible. Minor toxicokinetic differences can be addressed by genetically modifying test organisms to express enzymes that are crucial in human toxicokinetic pathways. MtCYP2E1 may be one of these crucial enzymes, though more research needs to be done to differentiate mtCYP2E1 from its microsomal counterpart and examine its specific effects in disease progression.

Monitoring global oxylipin production is a final tool that can measure the impact of CYP2E1 and xenobiotics on an organism's oxidative stress burden. There is ongoing

UPLC-MS/MS testing measuring the impact of paraquat exposure on global oxylipin production. This method is being optimized to produce signals above the instrument's LOD, but recent adjustments to the method show a 66% increase in oxylipin detection. Once it is optimized, rather than focusing on individual biomarkers that may not be significantly changed by oxidative stress, this method will monitor the production of dozens of oxylipins to show the impact of paraquat, styrene, and other xenobiotics on PUFA auto-oxidation and metabolism.

Pharmaceuticals are known to inhibit oxylipin pathways and shunt PUFAs down alternative oxylipin pathways, making global oxylipin monitoring especially useful in testing xenobiotic-induced oxidative stress. For example, oxylipin-producing enzymes are key targets for the control of pain (by the COX pathway) and asthma (by the LOX pathway), making billions of dollars for the pharmaceutical industry annually [50, 51]. If the COX enzyme pathway is inhibited, dietary fatty acids are shunted down one of the other enzyme pathways, causing an increase in metabolites like EpFAs that reduce oxidative stress [93]. The decrease in COX metabolites coinciding with an increase in EpFAs would only be noticed if many oxylipins are measured rather than a select few, meaning that global oxylipin monitoring is essential in measuring the complete impact of xenobiotic-induced oxidative stress. Not only will this oxylipin method provide a mechanistic overview of the oxidative stress response, it will also show the impact of oxidative stress on enzyme regulation without relying on reliable patterns of gene expression (something that is often relied upon in traditional oxidative stress tests).

These data will help clarify which oxylipin-signalling pathways influence the oxidative stress response in the mitochondria and the ER, which, along with traditional

oxidative stress testing, could help determine how the cellular localization of CYP2E1 affects oxidative stress, mitochondrial dysfunction, and toxicity.

5.0 Bibliography

[1] H. Sies, C. Berndt and D. P. Jones, "Oxidative Stress," *Annual Review of Biochemistry,* vol. 86, pp. 715-748, 2017.

[2] S. Mena, A. Ortega and J. Estrela, "Oxidative stress in environmental-induced carcinogenesis," *Mutation Research,* vol. 674, pp. 36-44, 2009.

[3] J. A. Harvilchuck, X. Pu, J. E. Klaunig and G. P. Carlson, "Indicators of oxidative stress and apoptosis in mouse whole lung and Clara cells following exposure to styrene and its metabolites," *Toxicology,* vol. 264, no. 3, pp. 171-178, 2009.

[4] C. Berry, C. La Vecchia and P. Nicotera, "Paraquat and Parkinson's disease," *Nature,* vol. 17, pp. 1115-1125, 2010.

[5] S. McCarthy, M. Somayajulu, M. Sikorska, H. Borowy-Borowski and S. Pandey, "Paraquat induces oxidative stress and neuronal cell death: neuroprotection by water-soluble Coenzyme Q10," *Toxicology and Applied Pharmacology,* vol. 201, no. 1, pp. 21-31, 2004.

[6] A. L. McCormack, J. G. Atienza, L. C. Johnston, J. K. Andersen, S. Vu and D. A. Di Monte, "Role of oxidative stress in paraquat-induced dopaminergic cell degeneration," *Journal of Neurochemistry,* vol. 93, no. 4, pp. 1030-1037, 2005.

[7] M. J. Davies, "Protein oxidation and peroxidation," *Biochemical Journal,* vol. 473, no. 7, pp. 805-825, 2016.

[8] H. J. Forman, M. Maiorino and F. Ursini, "Signaling Functions of Reactive Oxygen Species," *Biochemistry,* vol. 49, no. 5, pp. 835-842, 2010.

[9] J. P. Kehrer, "The Haber–Weiss reaction and mechanisms of toxicity," *Toxicology,* vol. 149, no. 1, pp. 43-50, 2000.

[10] C. C. Winterbourn, "Toxicity of iron and hydrogen peroxide: the Fenton reaction," *Toxicology Letters,* Vols. 82-83, pp. 969-974, 1995.

[11] J. S. Bus and J. E. Gibson, "Paraquat: model for oxidant-initiated toxicity," *Environmental Health Perspectives,* vol. 55, pp. 37-46, 1984.

[12] A. T. Black, J. P. Gray, M. P. Shakarjian, D. P. Laskin, D. E. Heck and J. D. Laskin, "Increased oxidative stress and antioxidant expression in mouse keratinocytes following exposure to paraquat," *Toxicology and Applied Pharmacology,* vol. 231, no. 3, pp. 384-392, 2008.

[13] Q. Hu, D. R. D'Amora, L. T. MacNeil, A. J. M. Walhout and T. J. Kubiseski, "The oxidative stress response in Caenorhabditis elegans requires the GATA factor ELT-3 and SKN-1/Nrf2," *Genetics,* vol. 206, no. 4, pp. 1909-1922, 2017.

[14] A. Amici, R. L. Levine, L. Tsai and E. R. Stadtman, "Conversion of amino acid residues in proteins and amino acid homopolymers to carbonyl derivatives by metal-catalyzed oxidation reactions," *Journal of Biological Chemistry,* vol. 264, no. 6, pp. 3341-3346, 1989.

[15] P. A. Grimsrud, H. Xie, T. J. Griffin and D. A. Bernlohr, "Oxidative stress and covalent modification of protein with bioactive aldehydes," *Journal of Biological Chemistry,* vol. 283, no. 32, pp. 21837-21841, 2008.

[16] A. Ayala, M. F. Muñoz and S. Argüelles, "Lipid peroxidation: production, metabolism, and signaling mechanisms of malondialdehyde and 4-hydroxy-2-nonenal," *Oxidative Medicine and Cellular Longevity,* vol. 2014, p. 360438, 2014.

[17] Y. Dotan, D. Lichtenberg and I. Pinchuk, "Lipid peroxidation cannot be used as a universal criterion of oxidative stress," *Progress in Lipid Research,* vol. 43, no. 3, pp. 200-227, 2004.

[18] R. J. Schaur, W. Siems, N. Bresgen and P. M. Eckl, "4-Hydroxy-nonenal—a bioactive lipid peroxidation product," *Biomolecules,* vol. 5, no. 4, pp. 2247-2337, 2015.

[19] C. Schneider, K. A. Tallman, N. A. Porter and A. R. Brash, "Two distinct pathways of formation of 4-hydroxynonenal," *Journal of Biological Chemistry,* vol. 276, no. 24, pp. 20831-20838, 2001.

[20] J. S. Walsh and G. T. Miwa, "Bioactivation of drugs: risk and drug design," *Annual Review of Pharmacology and Toxicology,* vol. 51, pp. 145-167, 2011.

[21] J. E. Laine, S. Auriola, M. Pasanen and R. O. Juvonen, "Acetaminophen bioactivation by human cytochrome P450 enzymes and animal microsomes," *Xenobiotica,* vol. 39, no. 1, pp. 11-21, 2009.

[22] M. R. McGill, M. R. Sharpe, C. D. Williams, M. Taha, S. C. Curry and H. Jaeschke, "The mechanism underlying acetaminopheninduced hepatotoxicity in humans and mice involves mitochondrial damage and nuclear DNA fragmentation," *Journal of Clinical Investigation,* vol. 122, no. 4, pp. 1574-1583, 2012.

[23] G. Wei, A. Bergquist, U. Broomé, S. Lindgren, S. Wallerstedt, S. Almer, P. Sangfelt, Å. Danielsson, H. Sandberg-Gertzén, L. Lööf and E. Björnsson, "Acute liver failure in

Sweden: etiology and outcome," *Journal of Internal Medicine,* vol. 262, no. 3, pp. 393-401, 2007.

[24] A. Dey, Cytochrome P450 2E1: its role in disease and drug metabolism, Dordrecht: Springer Netherlands, 2013.

[25] F. J. Gonzalez, "Role of cytochromes P450 in chemical toxicity and oxidative stress: studies with CYP2E1," *Mutation Research,* vol. 569, pp. 101-110, 2005.

[26] J. H. Hartman, G. Boysen and G. P. Miller, "CYP2E1 Metabolism of Styrene Involves Allostery," *Drug Metabolism and Disposition,* vol. 40, no. 10, pp. 1976-1983, 2012.

[27] D. R. Koop, "Alcohol metabolism's damaging effects on the cell - A focus on reactive oxygen generation by the enzyme cytochrome P450 2E1," *Alcohol Research and Health,* vol. 29, no. 4, pp. 274-280, 2006.

[28] G. P. Carlson, "Metabolism and toxicity of styrene in microsomal epoxide hydrolase-deficient mice," *Journal of Toxicology and Environmental Health, Part A,* vol. 73, no. 24, pp. 1689-1699, 2010.

[29] J. H. Hartman, G. P. Miller and J. N. Meyer, "Toxicological implications of mitochondrial localization of CYP2E1," *Toxicology Research,* vol. 6, pp. 273-289, 2017.

[30] M.-A. Robin, H. K. Anandatheerthavarada, G. Biswas, N. B. V. Sepuri, D. M. Gordon, D. Pain and N. G. Avadhani, "Bimodal targeting of microsomal CYP2E1 to mitochondria through activation of an N-terminal chimeric signal by cAMP-mediated Phosphorylation," *Journal of Biological Chemistry,* vol. 277, no. 43, pp. 40583-40593, 2002.

[31] M.-A. Robin, H. K. Anandatheerthavarada, J.-K. Fang, M. Cudic, L. Otvos and N. G. Avadhani, "Mitochondrial targeted cytochrome P450 2E1 (P450 MT5) contains an intact N-terminus and requires mitochondrial specific electron transfer proteins for activity," *Journal of Biological Chemistry,* vol. 276, no. 27, p. 24680–24689, 2001.

[32] J. H. Hartman, H. C. Martin, A. A. Caro, A. R. Pearce and G. P. Miller, "Subcellular localization of rat CYP2E1 impacts metabolic efficiency toward common substrates," *Toxicology,* vol. 338, pp. 47-58, 2015.

[33] L. Knockaert, V. Descatoire, N. Vadrot and B. Fromenty, "Mitochondrial CYP2E1 is sufficient to mediate oxidative stress and cytotoxicity induced by ethanol and acetaminophen," *Toxicology in Vitro,* vol. 25, pp. 475-484, 2011.

[34] F. W.-Y. Wong, W.-Y. Chan and S. S.-T. Lee, "Resistance to carbon tetrachloride-induced hepatotoxicity in mice which lack CYP2E1 expression," *Toxicology and Applied Pharmacology,* vol. 153, pp. 109-118, 1998.

[35] V. T. Cheshchevik, E. A. Lapshina, I. K. Dremza, S. V. Zabrodskaya, R. J. Reiter, N. I. Prokopchik and I. B. Zavodnik, "Rat liver mitochondrial damage under acute or chronic carbon tetrachloride-induced intoxication: Protection by melatonin and cranberry flavonoids," *Toxicology and Applied Pharmacology,* vol. 261, pp. 271-279, 2012.

[36] J. H. Hartman, G. P. Miller, A. A. Caro, S. D. Byrum, L. M. Orr, S. G. Mackintosh, A. J. Tackett, L. A. MacMillan-Crow, L. M. Hallberg, B. T. Ameredes and G. Boysen, "1,3-butadiene-induced mitochondrial dysfunction is correlated with mitochondrial

CYP2E1 activity in collaborative cross mice," *Toxicology (Amsterdam),* vol. 378, pp. 114-124, 2017.

[37] J.-M. Ahn, H.-J. Eom, X. Yang, J. N. Meyer and J. Choi, "Comparative toxicity of silver nanoparticles on oxidative stress and DNA damage in the nematode, Caenorhabditis elegans," *Chemosphere,* vol. 108, pp. 343-352, 2014.

[38] B. Dilberger, S. Baumanns, F. Schmitt, T. Schmiedl, M. Hardt, U. Wenzel and G. P. Eckert, "Mitochondrial oxidative stress impairs energy metabolism and reduces stress resistance and longevity of C. elegans," *Oxidative Medicine and Cellular Longevity,* vol. 2019, p. 6840540, 2019.

[39] D.-E. Jeong, Y. Lee and S.-J. V. Lee, "Western blot analysis of C. elegans proteins," in *Hypoxia: Methods and Protocols*, New York, Humana Press, 2018, pp. 213-225.

[40] S. Luo and N. B. Wehr, "Protein carbonylation: avoiding pitfalls in the 2,4-dinitrophenylhydrazine assay," *Communications in Free Radical Research,* vol. 14, no. 4, pp. 159-166, 2009.

[41] P. Wang and S. R. Powell, "Decreased sensitivity associated with an altered formulation of a commercially available kit for detection of protein carbonyls," *Free Radical Biology and Medicine,* vol. 49, no. 2, pp. 119-121, 2010.

[42] L. Xie, R. Pandey, B. Xu, G. Tsaprailis and Q. M. Chen, "Genomic and proteomic profiling of oxidative stress response in human diploid fibroblasts," *Biogerontology,* vol. 10, no. 2, pp. 125-151, 2009.

[43] C.-S. Chen and H. Zhu, "Protein Microarrays," *Biotechniques,* vol. 40, no. 4, pp. 423-429, 2006.

[44] B. Halliwell and J. M. C. Gutteridge, "Measurement of reactive species," in *Free Radicals in Biology and Medicine*, Oxford, Oxford University Press, 2015.

[45] V. Mavangira and L. M. Sordillo, "Role of lipid mediators in the regulation of oxidative stress and inflammatory responses in dairy cattle," *Research in Veterinary Science,* vol. 116, pp. 4-14, 2018.

[46] K. M. Rund, D. Heylmann, N. Seiwert, S. Wecklein, C. Oger, J.-M. Galano, T. Durand, R. Chen, F. Gueler, J. Fahrer, J. Bornhorst and N. H. Schebb, "Formation of trans-epoxy fatty acids correlates with formation of isoprostanes and could serve as biomarker of oxidative stress," *Prostaglandins and Other Lipid Mediators,* vol. 144, p. 106334, 2019.

[47] W. Chen, G. Zheng, S. Yang, W. Ping, X. Fu, N. Zhang, D. Wang and J. Wang, "CYP2J2 and EETs protect against oxidative stress and apoptosis in vivo and in vitro following lung ischemia/reperfusion," *Cellular Physiology and Biochemistry,* vol. 33, pp. 1663-1680, 2014.

[48] B. Inceoglu, A. Bettaieb, F. G. Haj, A. V. Gomes and B. D. Hammock, "Modulation of mitochondrial dysfunction and endoplasmic reticulum stress are key mechanisms for the wide-ranging actions of epoxy fatty acids and soluble epoxide hydrolase inhibitors," *Prostaglandins and Other Lipid Mediators,* vol. 133, pp. 68-78, 2017.

[49] X.-Z. Ding, R. Hennig and T. E. Adrian, "Lipoxygenase and cyclooxygenase metabolism: new insights in treatment and chemoprevention of pancreatic cancer," *Molecular Cancer,* vol. 2, p. 10, 2003.

[50] A. Rossi, C. Pergola, A. Koeberle, M. Hoffmann, F. Dehm, P. Bramanti, S. Cuzzocrea, O. Werz and L. Sautebin, "The 5-lipoxygenase inhibitor, zileuton, suppresses prostaglandin biosynthesis by inhibition of arachidonic acid release in macrophages," *British Journal of Pharmacology,* vol. 189, pp. 62-66, 2010.

[51] A. Blobaum and L. Marnett, "Structural and functional basis of cyclooxygenase inhibition," *Journal of Medicinal Chemistry,* vol. 50, pp. 1425-1441, 2007.

[52] K. M. Rund, A. I. Ostermann, L. Kutzner, J.-M. Galano, C. Oger, C. Vigor, S. Wecklein, N. Seiwert, T. Durand and N. H. Schebb, "Development of an LC-ESI(-)-MS/MS method for the simultaneous quantification of 35 isoprostanes and isofurans derived from the major n3- and n6-PUFAs," *Analytica Chimica Acta,* vol. 1037, pp. 63-74, 2018.

[53] B. Barnych, A. A. Rand, T. Cajka, K. S. S. Lee and B. D. Hammock, "Synthesis of cyclooxygenase metabolites of 8,9- epoxyeicosatrienoic acid (EET): 11- and 15-hydroxy 8,9-EETs," *Organic and Biomolecular Chemistry,* vol. 15, p. 4308, 2017.

[54] C. Cuyamendous, A. de la Torre, Y. Y. Lee, K. S. Leung, A. Guy, V. Bultel-Poncé, J.-M. Galano, J. C.-Y. Lee, C. Oger and T. Durand, "The novelty of phytofurans, isofurans, dihomo-isofurans and neurofurans: Discovery, synthesis and potential application," *Biochimie,* vol. 130, pp. 49-62, 2016.

[55] I. Dalle-Donne, R. Rossi, R. Colombo, D. Giustarini and A. Milzani, "Biomarkers of oxidative damage in human disease," *Clinical Chemistry,* vol. 52, no. 4, pp. 601-623, 2006.

[56] L. J. Janssen, "Isoprostanes: an overview and putative roles in pulmonary pathophysiology," *American Journal of Physiology - Lung Cellular and Molecular Physiology,* vol. 280, pp. L1067-L1082, 2001.

[57] J. Díaz-Castro, J. Florido, N. Kajarabille, S. Prados, C. de Paco, O. Ocon, M. Pulido-Moran and J. J. Ochoa, "A new approach to oxidative stress and inflammatory signaling during labour in healthy mothers and neonates," *Oxidative Medicine and Cellular Longevity,* vol. 2015, p. 178536, 2015.

[58] L. Minghetti, A. Greco, F. Cardone, M. Puopolo, A. Ladogana, S. Almonti, C. Cunningham, V. H. Perry, M. Pocchiari and G. Levi, "Increased brain synthesis of prostaglandin E2 and F2-isoprostane in human and experimental transmissible spongiform encephalopathies," *Journal of Neuropathology and Experimental Neurology,* vol. 59, no. 10, pp. 866-871, 2000.

[59] D. T. Walsh, V. H. Perry and L. Minghetti, "Cyclooxygenase-2 is highly expressed in microglial-like cells in a murine model of prion disease," *Glia,* vol. 29, no. 4, pp. 392-396, 2000.

[60] J. A. Martinez, J. Yang, B. C. Wertheim, D. J. Roe, A. Schriewer, P. Lance, D. S. Alberts, B. D. Hammock and P. A. Thompson, "Celecoxib use and circulating oxylipins in a colon polyp prevention trial," *PLOS One,* vol. 13, no. 4, p. e0196398, 2018.

[61] M. Otto, C. Bucher, W. Lie, M. Muller, T. Schmidt and M. Kardell, "12(S)-HETE mediates diabetes-induced endothelial dysfunction by activating intracellular endothelial cell TRPV1," *American Society for Clinical Investigation,* vol. 130, no. 9, pp. 4999-5010, 2020.

[62] A. M. Guo, A. S. Arbab, J. R. Falck, P. Chen, P. A. Edwards, R. J. Roman and A. G. Scicli, "Activation of vascular endothelial growth factor through reactive oxygen species mediates 20-hydroxyeicosatetraenoic acid-induced endothelial cell proliferation," *Journal of Pharmacology and Experimental Therapeutics,* vol. 321, no. 1, pp. 18-27, 2007.

[63] T. Ishizuka, J. Cheng, H. Singh, M. D. Vitto, V. L. Manthati, J. R. Falck and M. Laniado-Schwartzman, *Journal of Pharmacology and Experimental Therapeutics,* vol. 324, no. 1, pp. 103-110, 2008.

[64] A. L. Johnson, K. Z. Edson, R. A. Totah and A. E. Rettie, "Cytochrome P450 ω-hydroxylases in inflammation and cancer," *Advances in Pharmacology,* vol. 74, pp. 223-262, 2015.

[65] T. D. Penning, "Inhibitors of leukotriene A4 (LTA4) hydrolase as potential Anti-inflammatory agents," *Current Pharmaceutical Design,* vol. 7, pp. 163-179, 2001.

[66] P. Li, D. Y. Oh, G. Bandyopadhyay, W. S. Lagakos, S. Talukdar, O. Osborn, A. Johnson, H. Chung, M. Maris, J. M. Ofrecio, S. Taguchi, M. Lu and J. M. Olefsky, "LTB4 causes macrophage–mediated inflammation and directly induces insulin resistance in obesity," *Nature Medicine,* vol. 21, no. 3, pp. 239-247, 2015.

[67] E. Dvash, M. Har-Tal, S. Barak, O. Meir and M. Rubinstein, "Leukotriene C4 is the major trigger of stress-induced oxidative DNA damage," *Nature Communications,* vol. 11, no. 6, p. 10112, 2015.

[68] B. Inceoglu, S. L. Jinks, A. Ulu, C. M. Hegedus, K. Georgi, K. R. Schmelzer, K. Wagner, P. D. Jones, C. Morisseau and B. D. Hammock, "Soluble epoxide hydrolase

and epoxyeicosatrienoic acids modulate two distinct analgesic pathways," *Proceedings of the National Academy of Sciences of the United States of America,* vol. 105, no. 48, pp. 18901-18906, 2008.

[69] Y. Zhou, G.-Y. Sun, T. Liu, J.-X. Duan, H.-F. Zhou, K. S. Lee, B. D. Hammock, X. Fang, C.-X. Guan and J.-X. Jiang, "Soluble epoxide hydrolase inhibitor 1-trifluoromethoxyphenyl-3- (1-propionylpiperidin-4-yl) urea attenuates bleomycin-induced pulmonary fibrosis in mice," *Cell and Tissue Research,* vol. 363, no. 2, pp. 399-409, 2016.

[70] S. K. Goswami, B. Inceoglu, J. Yang, D. Wan, S. D. Kodani, C. A. T. da Silva, C. Morisseau and B. D. Hammock, "Omeprazole increases the efficacy of a soluble epoxide hydrolase inhibitor in a PGE_2 induced pain model," *Toxicology and Applied Pharmacology,* vol. 289, no. 3, pp. 419-427, 2015.

[71] J. D. Malhotra, H. Miao, K. Zhang, A. Wolfson, S. Pennathur, S. W. Pipe and R. J. Kaufman, "Antioxidants reduce endoplasmic reticulum stress and improve protein secretion," *Proceedings of the National Academy of Sciences of the United States of America,* vol. 105, no. 47, pp. 18525-18530, 2008.

[72] D. Eletto, E. Chevet, Y. Argon and C. Appenzeller-Herzog, "Redox controls UPR to control redox," *Journal of Cell Science,* vol. 127, no. 17, pp. 3649-3658, 2014.

[73] L. Liu, C. Chen, W. Gong, Y. Li, M. L. Edin, D. C. Zeldin and D. W. Wang, "Epoxyeicosatrienoic acids attenuate reactive oxygen species level, mitochondrial dysfunction, caspase activation, and apoptosis in carcinoma cells treated with arsenic

trioxide," *Journal of Pharmacology and Experimental Therapeutics,* vol. 339, no. 2, pp. 451-463, 2011.

[74] S. Zhang, F. Li, T. Zhou, G. Wang and Z. Li, "Caenorhabditis elegans as a useful model for studying aging mutations," *Frontiers in Endocrinology,* vol. 11, p. 554994, 2020.

[75] S. Brenner, "The genetics of Caenorhabditis elegans," *Genetics,* vol. 77, pp. 71-94, 1974.

[76] Z. F. Altun and D. H. Hall, "Introduction to C. elegans Anatomy," 24 April 2012. [Online]. Available: https://www.wormatlas.org/hermaphrodite/introduction/Introframeset.html. [Accessed 5 December 2021].

[77] A. K. Corsi, B. Wightman and M. Chalfie, "A transparent window into biology: a primer on Caenorhabditis elegans," The C. elegans Research Community, WormBook, 15 June 2015. [Online]. Available: http://www.wormbook.org. [Accessed 5 December 2021].

[78] E. L. L. Sonnhammer and R. Durbin, "Analysis of protein domain families in Caenorhabditis elegans," *Genomics,* vol. 46, pp. 200-216, 1997.

[79] R. H. Waterston, K. Lindblad-Toh, E. Birney, J. Rogers, J. F. Abril, P. Agarwal and e. al., "Initial sequencing and comparative analysis of the mouse genome," *Nature,* vol. 42, pp. 550-562, 2002.

[80] T. Stiernagle, "Maintenance of C. elegans," The C. elegans Research Community, WormBook, 6 February 2006. [Online]. [Accessed 5 December 2021].

[81] L. M. Katiki, J. F. Ferreira, A. M. Zajac, C. Masler, D. S. Lindsay, A. C. S. Chagas and A. F. T. Amarante, "Caenorhabditis elegans as a model to screen plant extracts andcompounds as natural anthelmintics for veterinary use," *Veterinary Parasitology,* vol. 182, pp. 264-268, 2011.

[82] J. R. Manjarrez and R. Mailler, "Stress and timing associated with Caenorhabditis elegans immobilization methods," *Heliyon,* vol. 6, p. e04263, 2020.

[83] Thermo Fisher Scientific, "Protein quantitation assay compatibility table," [Online]. Available: https://assets.thermofisher.com/TFS-Assets/LSG/Application-Notes/TR0068-Protein-assay-compatibility.pdf. [Accessed 03 02 2021].

[84] EMD Millipore Corporation, "OxyBlot Protein Oxidation Detection Kit," 2016. [Online]. Available: https://www.emdmillipore.com/Web-CA-Site/en_CA/-/CAD/ShowDocument-File?ProductSKU=MM_NF-S7150&DocumentId=201410.030.ProNet&DocumentUID=9534625&DocumentType=PI&Language=EN&Country=NF&Origin=PDP. [Accessed 02 03 2021].

[85] I. B. Slimen, T. Najar, A. Ghram, H. Dabbebi, M. B. Mrad and M. Abdrabbah, "Reactive oxygen species, heat stress and oxidative-induced mitochondrial damage. A review," *International Journal of Hyperthermia,* vol. 30, no. 7, pp. 513-523, 2014.

[86] L. Miao and D. K. St. Clair, "Regulation of superoxide dismutase genes: implications in diseases," *Free Radical Biology and Medicine,* vol. 47, no. 4, pp. 344-356, 2009.

[87] W. Yang, J. Li and S. Hekimi, "A measurable increase in oxidative damage due to reduction in superoxide detoxification fails to shorten the life span of long-lived

mitochondrial mutants of Caenorhabditis elegans," *Genetics,* vol. 177, no. 4, pp. 2063-2074, 2007.

[88] V. Yu, "Bead beating offers high-performance homogenization for molecular biology downstream processing of tough and difficult samples," in *Sample Preparation Techniques for Soil, Plant, and Animal Samples*, New York, NY: Humana Press, 2016, pp. 85-97.

[89] B. E. P. Saudia, K. M. Kisid, S. Andarini and E. Mustofa, "The effects of yoga exercise on lipid peroxidation and antioxidant status in pregnant women," *Indian Journal of Medical Specialities,* vol. 9, no. 2, pp. 65-68, 2018.

[90] D. Wang, Y. Ma, X. Yang, X. Xu, Y. Zhao, Z. Zhu, X. Wang, H. Deng, C. Li, F. Gao, J. Tong, K. Yamanaka and Y. An, "Hypermethylation of the Keap1 gene inactivates its function, promotes Nrf2 nuclear accumulation, and is involved in arsenite-induced human keratinocyte transformation," *Free Radical Biology and Medicine,* vol. 89, pp. 209-219, 2015.

[91] E. Possik and A. Pause, "Measuring oxidative stress resistance of Caenorhabditis elegans in 96-well microtiter plates," *Journal of Visualized Experiments,* vol. 99, p. e52746, 2015.

[92] C. J. Weydert and J. J. Cullen, "Measurement of superoxide dismutase, catalase and glutathione peroxidase in cultured cells and tissue," *Nature Protocols,* vol. 5, no. 1, pp. 51-66, 2010.

[93] T. R. Harris, S. Kodani, A. A. Rand, J. Yang, D. M. Imai, S. H. Hwang and B. D. Hammock, "Celecoxib does not protect against fibrosis and inflammation in a carbon

tetrachloride-induced model of liver injury," *Molecular Pharmacology,* vol. 94, pp. 834-841, 2018.

6.0 Supplementary Information

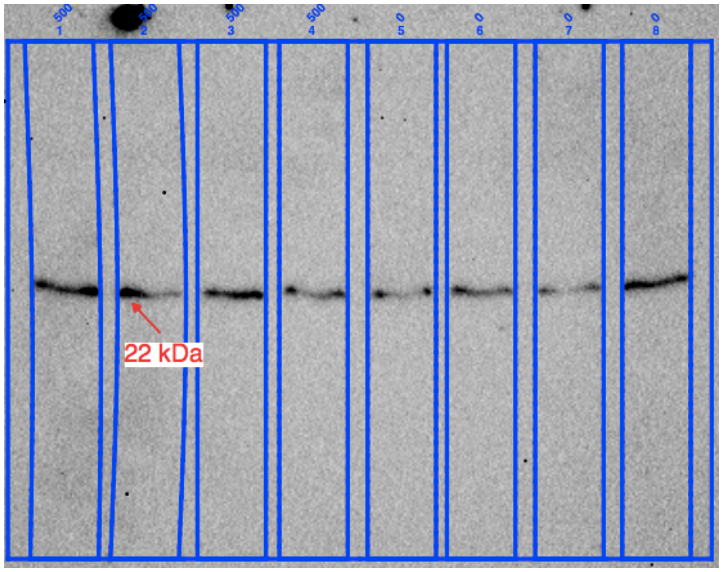

Figure S.1 Full image of the chemiluminescence of erCYP2E1 SOD-2 bands (22 kDa) incubated in 500 (lanes 1-4) and 0 (lanes 5-8) μM styrene in M9, then lysed by glass beads.

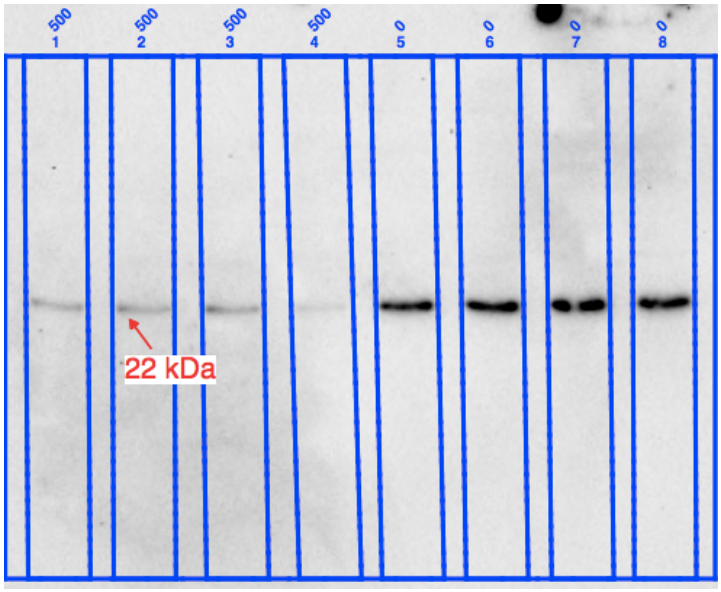

Figure S.2 Full image of the chemiluminescence of mtCYP2E1 SOD-2 bands (22 kDa) incubated in 500 (lanes 1-4) and 0 (lanes 5-8) μM styrene in M9, then lysed by glass beads.

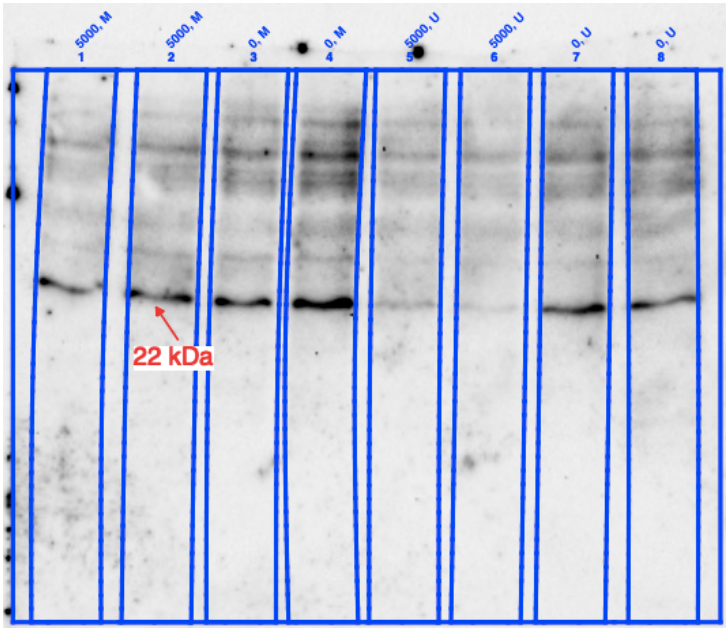

Figure S.3 Full image of the chemiluminescence of mtCYP2E1 SOD-2 bands (22 kDa) incubated in 5000 (lanes 1-2, 5-6) and 0 (lanes 3-4, 7-8) μM styrene in M9, then lysed by either mixed- (M) (lanes 1-4) or uniformly- (U) (lanes 5-8) sized ceramic beads.

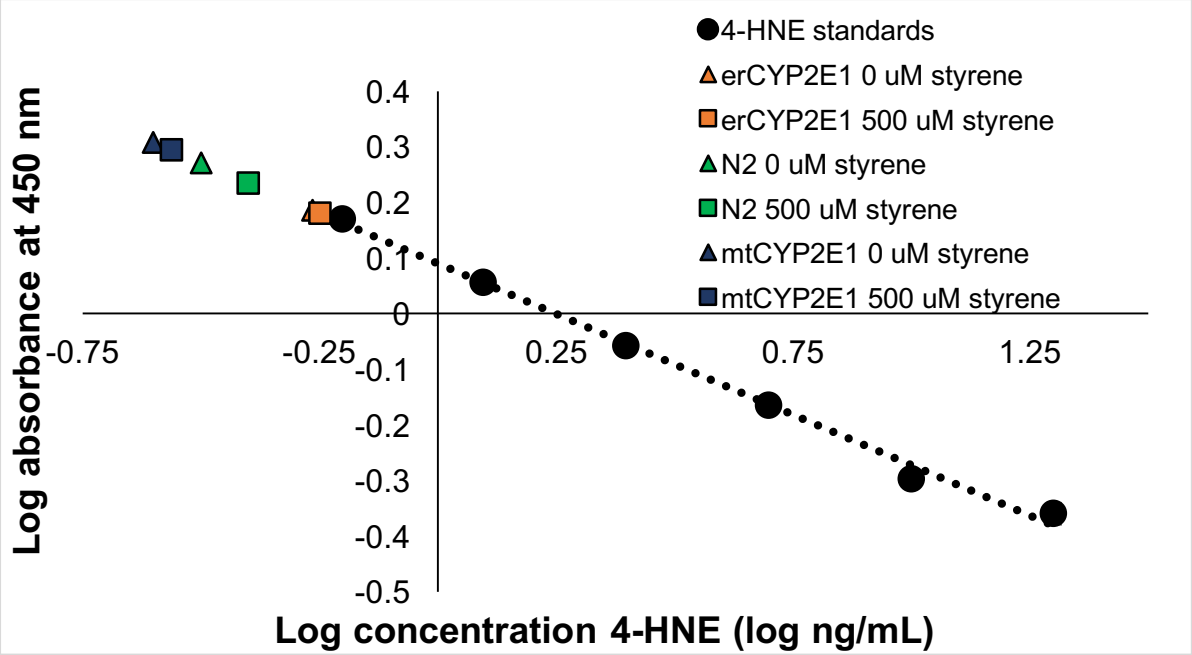

Figure S.4 OD450 of 4-HNE assay standards and styrene-exposed *C. elegans*, demonstrating that all samples were below the detection range of the competitive ELISA (0.63-40 ng/mL). The highest 4-HNE concentration was observed in styrene-exposed erCYP2E1 worms.

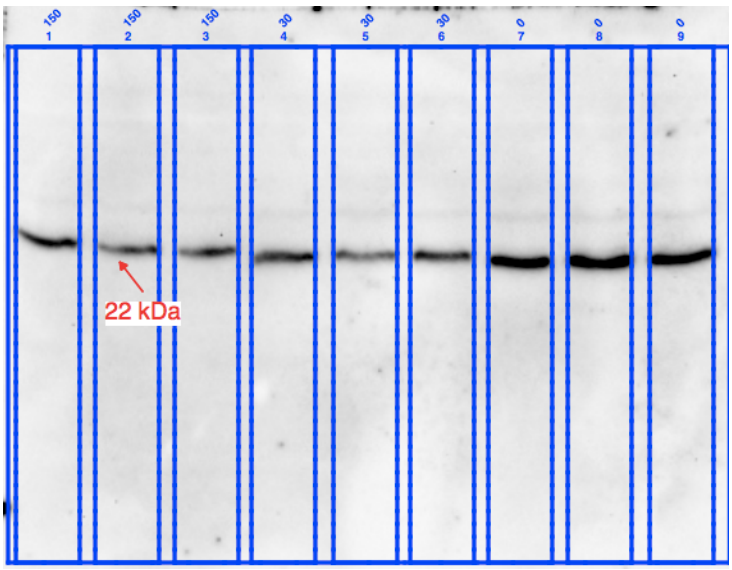

Figure S.5 Full image of the chemiluminescence of mtCYP2E1 SOD-2 bands (22 kDa) incubated in 150 (lanes 1-3), 30 (lanes 4-6), and 0 (lanes 7-9) mM paraquat in M9, then lysed by mixed-size ceramic beads.

Table S.1 Oxylipins and their parent PUFAs monitored in this study. The table contains 74 compounds (including 14 internal standards), their precursor and product ions, the optimized cone and collision energies, as well as retention time and the respective internal standard for correction.

Analyte	Precursor Ion (m/z)	Product Ion (m/z)	Cone (V)	CE (V)	RT (min)	Internal Standard
ARA	303.4	259.4	60	10	5.4	d11-LA
PGE_2	351.4	271.5	30	15	5	d14-PGE_2
d4-PGE_2	355.5	275.4	10	15	5	-
$PGF_{2\alpha}$	353.4	193.3	70	25	4.8	d4-PGF2a
d4-$PGF_{2\alpha}$	357.3	197.3	55	25	4.8	-
6-keto-PGF1a	369.4	163.4	50	25	4.1	d4-PGF2a
TXB_2	369.4	169.2	10	15	4.6	d4-TXB_2
d4-TXB_2	373.3	199.3	20	15	4.6	-
8,9-EET	319.5	155.1	50	10	15.5	d11-11,12-EET
11,12-EET	319.1	167.2	40	15	12.3	d11-11,12-EET
d11-11,12-EET	**330.2**	**167.1**	**30**	**10**	**15**	-
14,15-EET	319.4	219.3	30	10	14.4	d11,11,12-EET
8,9-DiHETrE	337.3	127.2	20	20	9.4	d11-14,15-DHET
11,12-DiHETrE	337.4	167.4	25	15	8.8	d11-14,15-DHET
14,15-DiHETrE	337.4	207.2	25	15	8.2	d11-14,15-DHET
d11-14,15-DHET	**348.5**	**207.4**	**25**	**15**	**8.1**	-
5-Iso-$PGF_{2\alpha}$-VI	353.5	115.2	50	20	4.8	d4-PGF2a
5-HETE	319.3	257.5	40	10	13.6	d8-15-HETE
8-HETE	319.2	155.2	30	10	12.8	d8-15-HETE

9-HETE	319.2	155.2	20	15	12.4	d8-15-HETE
11-HETE	319.2	167.2	20	15	12.3	d8-15-HETE
12-HETE	319.2	179.2	25	20	12.8	d8-15-HETE
15-HETE	319.4	219.2	10	10	11.7	d8-15-HETE
d8-15-HETE	327.3	182.6	15	15	11.5	**-**
20-HETE	319.3	275.3	50	15	9.9	d6-20-HETE
d6-20-HETE	**325.3**	**281.4**	**35**	**15**	**9.8**	-
5-OxoETE	317.7	203.2	50	20	14.4	d8-15-HETE
15-OxoETE	317.2	113.1	20	15	11.7	d8-15-HETE
Lipoxin A4	351.3	115.4	30	15	5.6	d4-LKB4
LKB4	335.2	195.3	40	15	7.3	d4-LKB4
d4-LKB4	**339.4**	**197.2**	**40**	**15**	**7.3**	**-**
LXD4	495.3	177.3	60	20	5.5	d4-LKB4
LA	279.4	261.3	40	15	5.5	d11-LA
d11-LA	290.4	272.3	30	20	5.5	**-**
9,10-EpOME	295.3	171.1	55	15	14.5	d4-9,10-EpOME
d4-9,10-EpOME	**299.2**	**172.3**	**60**	**15**	**14.4**	**-**
12,13-EpOME	295.3	195.2	45	15	14.2	d4-9,10-EpOME
9,10-DiHOME	313.3	201.2	30	20	7.9	d4-12,13-diHOME
12,13-DiHOME	313.3	183.3	60	20	7.5	d4-12,13-diHOME
d4-12,13-DiHOME	317.1	185.3	40	20	7.5	**-**
9-HODE	295.3	171.3	30	15	11.3	d4-9-HODE
d4-9-HODE	299.2	172.3	35	15	11.2	**-**
13-HODE	295.3	195.2	50	15	11.1	d4-9-HODE
9-OxoODE	293.4	185.2	40	20	12.7	d3-9-oxoODE
d3-9-oxoODE	296.3	296.5	50	20	12.5	**-**
13-OxoODE	293.3	113.2	70	20	12	d3-9-oxoODE
DHA	327.2	283.4	25	10	5.2	d5-DHA
d5-DHA	332.3	288.4	10	10	5.2	**-**
7,8-EpDPE	343.1	189.3	15	10	15.5	d11-11,12-EET
16,17-EpDPE	343.2	233.2	20	10	14.6	d11-11,12-EET
19,20-EpDPE	343.3	281.3	25	10	13.9	d11-11,12-EET
7,8-DiHDPA	361.4	113.3	40	15	12.8	d11-14,15-DHET
16,17-DiHDPA	361.3	233.4	40	15	12.2	d11-14,15-DHET
19,20-DiHDPA	361.4	273.4	25	15	11.7	d11-14,15-DHET
4-HDHA	343.0	101.1	20	15	13.3	d8-15-HETE
14-HDHA	343.3	281.5	10	10	12.4	d8-15-HETE
16-HDHA	343.5	233.3	15	10	11.7	d8-15-HETE
17-HDHA	343.4	281.3	20	10	11.9	d8-15-HETE
20-HDHA	343.2	241.5	20	10	10.5	d6-20-HETE
Resolvin D1	375.3	141.5	20	15	5.5	d4-LKB4
EPA	301.4	257.4	30	10	4.9	d5-EPA
d5-EPA	306.2	262.4	30	10	4.9	**-**

PGE3	349.2	269.2	20	15	4.6	d14-PGE_2
8,9-EpETE	317.2	255.4	45	10	13	d11-11,12-EET
11,12-EpETE	317.3	167.4	15	10	12.8	d11-11,12-EET
14,15-EpETE	319.0	219.3	30	10	14.4	d11-11,12-EET
8,9-DiHETE	335.3	127.3	30	20	7.7	d11-14,15-DHET
11,12-DiHETE	335.2	167.3	30	15	7.4	d11-14,15-DHET
14,15-DiHETE	335.3	207.3	30	15	7.3	d11-14,15-DHET
5-HEPE	317.3	5.5	10	10	11.1	d8-15-HETE
8-HEPE	317.4	155.2	30	10	10.4	d8-15-HETE
12-HEPE	317.2	179.3	10	10	10.5	d8-15-HETE
15-HEPE	317.2	219.4	10	10	10	d8-15-HETE
18-HEPE	317.0	215.0	10	20	8.9	d6-20-HETE

Table S.2 Test comparing the difference in survival rates of N2, erCYP2E1, and mtCYP2E1 worms exposed to paraquat. P-values were calculated using one-way analysis of variance where alpha = 0.050. Pairwise multiple comparison procedures were completed using the Holm-Sidak method.

Paraquat concentration (mM)	**Pass (P) or Fail (F)**	**P-value**
0	P	0.811
10	P	0.835
25	P	0.473
50	F	0.029*
100	P	0.170
250	F	0.040**
500	P	0.413

*, survival significantly ($p<0.05$) decreased in mtCYP2E1 worms relative to N2 worms

**, there was no significant difference in survival between individual worm strains